Deadbeat Current Control in Grid-Connected Inverters: A Comprehensive Discussion

GARBA ELHASSAN[1,2], **SHAMSUL AIZAM ZULKIFLI**[1],
SOLOMON ZAKWOI ILIYA[2,3], (Member, IEEE),
HASSAN BEVRANI[4], (Senior Member, IEEE),
MOMOH KABIR[1], **RONALD JACKSON**[1],
MUBASHIR HAYAT KHAN[1],
AND MOHAMMED AHMED[5]

[1]Department of Electrical Power Engineering, Faculty of Electrical and Electronic Engineering, Universiti Tun Hussein Onn Malaysia (UTHM), Batu Pahat, Parit Raja, Johor 86400, Malaysia
[2]National Space Research and Development Agency, Obasanjo Space Centre, Lugbe, Abuja 9000107, Nigeria
[3]Institute of Space Science and Engineering, African University of Science and Technology, Galadimawa, Abuja 900109, Nigeria
[4]Department of Electrical and Computer Engineering, University of Kurdistan, Sanandaj, Kurdistan 66177-15175, Iran
[5]Department of Electrical Engineering, Abubakar Tafawa Balewa University, Bauchi 740272, Nigeria

Corresponding authors: Garba Elhassan (ge180033@siswa.uthm.edu.my) and Shamsul Aizam Zulkifli (aizam@uthm.edu.my)

ABSTRACT Discrete-time dynamic systems demonstrate quite exciting possibilities from the perspective of control as compared with the continuous-time counterpart. Interesting properties of discrete-time dynamic systems include the possibility to algebraically determine previously unknown system parameters by simply measuring the present inputs and outputs of the system. Additionally, achieving a finite settling time with zero steady-state error is only achievable in discrete-time dynamic systems. Deadbeat current control (DBCC) has been used to achieve a finite settling time, especially in grid-connected inverter applications. However, there is no comprehensive study on reviewing or evaluating existing control approaches, to the authors' best knowledge. This paper systematically examined the existing methods by paying attention to four key research issues: 1) research evidence indicating the adoption of DBCC in grid-connected inverter applications (GCIAs), 2) the types of deadbeat control approaches adopted in GCIAs, 3) the best approach in terms of stability especially regarding grid-impedance variation, and 4) the barriers that might prevent the wide adoption of DBCC in GCIAs. Finally, this paper presents a hypothesis based on the simulated results on which approach is superior at present to give readers a direction for further research classification on deadbeat control.

INDEX TERMS Deadbeat control, grid-connected inverter, current control, renewable energy sources.

I. INTRODUCTION

The continuously increasing demand for electrical energy globally has instituted the need to harness other sources of energy. The liberalization of the grid has resulted in various changes in the operation and control of power systems, which include stability assurances, quality assurance of the injected energy, safety measures both at the energy source units and at the consumer's end, and a requirement for fault tolerance and islanded mode requirement, to mention but a few [1]. Power electronics inverters (PEIs) form a bridge between the

The associate editor coordinating the review of this manuscript and approving it for publication was Engang Tian.

renewable energy generated and the distributed generation systems (DGSs). But due to the intermittent nature of the primary energy source, there is a need to build a robust control system for PEIs to meet the standard required for grid-connected and stand-alone modes.

The control can cover the voltage, current, power, or a hybrid of any of these variables in a cascaded loop in the form of either an inner-loop or outer-loop control structure. The inner current control is employed in many research works to ensure accurate current tracking, adequate control bandwidth and fast transient response [2]. In a voltage-source inverter (VSI), a current controller is employed to make the inverter act as a current amplifier within the current-loop

bandwidth [3], but in the case of an outer-loop structure, a voltage controller is employed to ensure power flow operation in the system by rejecting disturbances from both the input sources and the grid.

Renewable energy sources supplying power to the grid via grid voltage-source inverter inject distorted current into the primary grid; therefore, its harmonics content must be contained to meet the grid standard [4]. Some of the sources of current harmonics include grid voltage distortion and the non-linearity of the power inverter, which can be mitigated by choosing a proper control technique. Additionally, the switching ripple of the inverter adds high-frequency ripples to the current waveform, which can be mitigated by using a passive L or LCL filter at the output of the inverter [5]. These two control approaches are available depending on where the sensor is placed (inverter side or grid side), and the use of current sensor(s) has become mandatory to protect the system against overcurrent instances. When an LCL filter is adopted to mitigate the switching harmonics at the inverter's output, the sensor can be placed either at the inverter side or at the grid side. For overcurrent protection, the sensor is placed at the inverter side because current dynamics are filtered faster at this side. To avoid the cost of using two or more sensors, which is the case for grid-side control, an alternative is to use the inverter-side control, which needs a single sensor for both overcurrent protection and control purposes. Therefore, fast overcurrent protection and a good stability margin can be achieved using the inverter-side control compared with the grid-side control [4].

The control either at the inverter side or the grid side can be implemented either in a continuous or a discrete domain.

Discrete-time dynamic systems demonstrate quite exciting possibilities regarding control as compared with the continuous-time counterpart. Interesting properties of discrete-time dynamic systems include the option to algebraically determine previously unknown system parameters by merely measuring the present inputs and outputs of the system, assuming that the measuring environment is noise-free. However, supposing that the measuring environment is characterized by some associated noises, then the procedure of the algebraic determination of previously unknown system parameters can be extended by closed-form optimization using one of the least-squares techniques [6]. This method of obtaining unknown system parameters is called system identification [7]. Therefore, using the obtained and measured system parameters, it is possible to obtain a finite settling time with zero steady-state error from a given input reference signal by canceling the polynomials, which represent the system's dynamics. This balancing is achieved through a feedback compensation technique referred to as deadbeat control (DBC).

Alternatively, finite settling time and input signal tracking can be achieved if the system parameters are known by subtracting the system dynamics geometrically via a feedback compensation technique referred to as one-step-ahead control. However, this technique is associated with a one-step delay between the input and output signals. Furthermore, deadbeat and one-step-ahead control techniques are achievable only in a discrete form. The parameters are described by the difference equation that algebraically relates to the system's input and output signals. On the contrary, a continuous system is defined by differential equations. DBC is not achievable for linear time-invariant feedback because the error exponentially decays and vanishes only as time goes to infinity. Deadbeat and N-steps-ahead controls were researched separately in the past, but the two ideas were later merged and called DBC [6].

Control in PEIs is currently implemented digitally on a microprocessor due to advances in digital signal processing. Several problems are associated with the digital implementation, which are unique to the system and would limit its performance and capabilities. These include the presence of time delay, which changes the controller's phase-frequency characteristic, and the tendency of instability, the presence of ripple component at the sampling frequency, the presence of the harmonics in the output, and the restriction on the usable bandwidth to a fraction of the sampling frequency [8]. However, for specific applications, digital controllers have demonstrated good advantages, which outweigh the disadvantages mentioned above to the extent that digital control systems are more desirable. Such applications where digital control can be most desirable include large process controls, industrial drives and regulators, renewable power generations, etc. Therefore, research on digital controllers is now gaining attention from many researchers all over the world.

Among digital controllers, deadbeat current controller (DBCC) has gained serious attention for decades because of its advantages, such as zero steady-state error [9], [10], easy implementation on a digital control system, low current harmonics, fast dynamic response [11] and robust time-delay compensation [12]. It should be noted that the desired class of input signal must be specified before designing a controller that will achieve a response with finite settling time. Consequently, there is no clear understanding of what precisely DBC is all about, based on the different perceptions that researchers have on the topic. It is worth noting that there are two basic design approaches to DBC. In the first case, all components that make up the system are subject to only digital data. In the second case, the components encompass both continuous and discrete components, and this is usually referred to as a sampled-data control system. In the case of all-digital data, there will be no issue of inter-sampling ripples, while for the sampled data, the issue of inter-sampling ripples has to be taken care of. To clarify the perception regarding this topic, based on our extensive reading of the literature, DBC can be broadly classified into six groups: pole-zero cancellation approach (PZCA), factorization approach (FRA), state-variable derivation approach (SVDA), hybrid design approach (HBDA), robust control approach (RCA) and other DBC design approaches (ODA), as shown in Figure 1.

The remainder of this paper is organized as follows: I, data analysis from selected papers is presented in
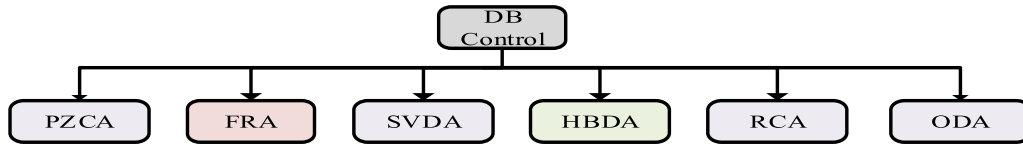
FIGURE 1. Types of DBC.

TABLE 1. Research questions and their reasons.

S/No.	Research questions	Reason for choosing the question
1	What research evidence indicates the adoption of DBCC in GCIAs?	This question was designed to collect all relevant existing research findings within the specified period to organize and classify the research into an ordered format. It would provide a clear and explicit overview of the current body of knowledge.
2	What are the types of DBC approaches adopted in GCIAs?	This question was designed to divulge the existing approaches in designing a deadbeat controller, alongside the impressive achievement so far reported in the current body of knowledge.
3	Which of the approaches is best in terms of stability, especially with regard to grid-impedance variation?	This question was designed to guide the readers in selecting the best approach out of those considered in this research work.
4	What are the barriers that may prevent the wide adoption of DBCC in GCIAs?	This question was designed to reveal any underlining issues faced by GCI when adopting the DBCC technique.

Note: DBC: Deadbeat Control, DBCC: Deadbeat Current Control, GCI: Grid-Connected Inverter, GCIA: Grid-Connected Inverter Application

Section II, comparison of some control strategies is presented in Section III. Lastly, a conclusion is presented in Section IV.

II. DATA ANALYSIS FROM SELECTED PAPERS

This research's initial query returned 250 articles: 32 articles from IEEE Xplore, 137 articles from Scopus and 81 articles from Engineering Village, all of which were from the year 2000 to 2021. Based on the original output, 49 articles were found to be duplicates and were removed. After scanning the articles and abstracts, another 49 articles were excluded from the total. Additionally, after in-depth reading and criteria application, 51 articles were excluded, leaving a total of 101 articles. After data synthesis, a total of 54 papers were finally considered. The research methodology advocated in [13], [14] was adopted in this research work with details of the research questions tabulated in Table 1.

A. RQ1: WHAT RESEARCH EVIDENCE INDICATES THE ADOPTION OF DBCC IN GCIAs?

To address the first research question, a literature classification was created. The final 54 papers were read and studied to obtain a detailed picture and the research subject's perception. The overall research was classified into four groups, as earlier discussed. Figure 2 shows the papers' breakdown by sources, with IEEE Xplore having the highest number of papers, while in Figure 3, it is clear that 70% of the papers under consideration were journal papers and 30% were conference papers. This study observed each research category and studied the findings to produce a comprehensive taxonomy. It is worth

noting that some of the papers were not as clearly defined as suggested and some overlapped into different subcategories. In general, the result of RQ1 shows the adoption of DBC is increasing in GCI applications and is continuously attracting many researchers, as indicated in Figure 4.
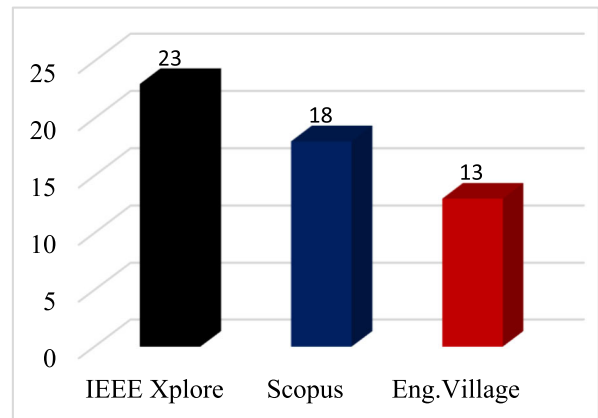

FIGURE 2. Data sources.

B. RQ2: WHAT ARE THE TYPES OF DBC APPROACHES ADOPTED IN GCIAs?

To address the second research question, DBC approaches are classified into six groups based on our intensive reading of the literature, and the basic approaches to achieving each are discussed below:
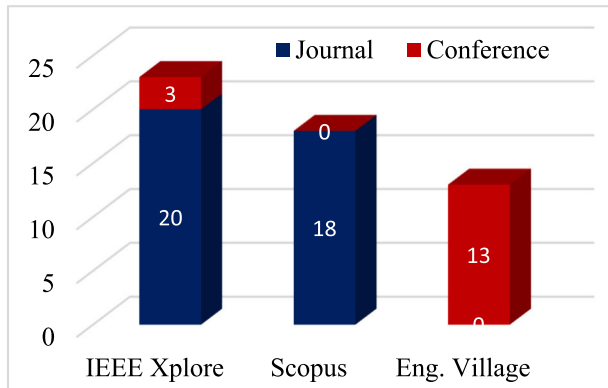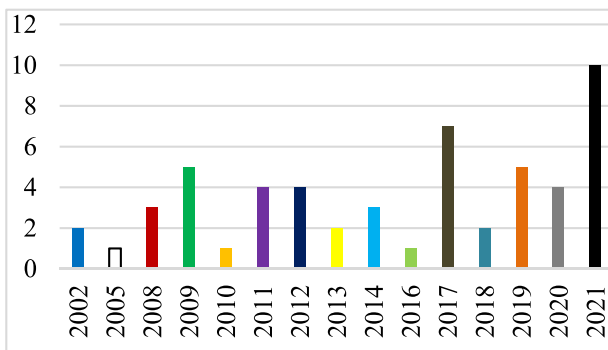
FIGURE 3. Breakdown of publications by type.

FIGURE 4. Number of publications by year.

1) POLE-ZERO CANCELLATION APPROACH

The fundamental idea of this type of deadbeat controller is to prescribe a closed-loop transfer function of a unique form where all the poles of the closed-loop transfer function coincide at $z = 0$. Assuming the discrete plant transfer function to be $T(z)$ and the deadbeat controller to be $DB_{pzc(z)}$, applying these two into a standard closed loop, as shown in Figure 5, will yield a transfer function as in Equation 1:

$$N_{(z)} = \frac{DB_{pzc(z)} \times T_{(z)}}{1 + DB_{pzc(z)} \times T_{(z)}} \quad (1)$$

Equation 1 represents the prescribed special transfer function from the reference input ($R_{(z)}$) to the measured output ($C_{(z)}$). Therefore, Equation 1 can be re-written as:

$$N_{(z)} = \frac{Y_{(z)}}{E_{(z)}} = \frac{DB_{pzc(z)} \times T_{(z)}}{1 + DB_{pzc(z)} \times T_{(z)}} \quad (2)$$

From Equation 2, making $DB_{(z)}$ the subject yields:

$$DB_{p(z)} = \frac{1}{T_{(z)}} \times \frac{N_{(z)}}{1 - N_{(z)}} \quad (3)$$

The control in Equation 3 suggests a complete cancellation of plant $T(z)$. Therefore, to avoid unstable pole-zero cancellation, the plant is assumed to be stable and at the minimum phase. To achieve minimum-time deadbeat control, the desired closed-loop transfer functions are described as $N_{(z)} = \frac{1}{Z^n}$ and $N_{(z)} = \frac{Z-n}{Z^{n+1}}$ for step and ramp input signals,

respectively, where n represents the difference between the poles and zeros of the plant transfer function. For a non-minimum-phase system, $N_{(z)}$ and $1 - N_{(z)}$ are modified into Equations 4 and 5 as:

$$N_{(z)} = \prod_{i=1}^{k} \left(1 - z_i z^{-1}\right)$$
$$\times \left(m_k z^{-k} + m_{k+1} z^{-k-1} + \ldots m_{k+n} z^{-k-n}\right) \quad (4)$$

$$1 - N_{(z)} = \prod_{j=1}^{l} \left(1 - p_i z^{-1}\right) \left(1 - z^{-1}\right)^P$$
$$\times \left(1 + q_l z^{-l} + q_{l+1} z^{-l-1} + \ldots q_{l+n} z^{-l-n}\right) \quad (5)$$

where p depends on the order of the input signal or the order of the plant's poles at $z = 1$.
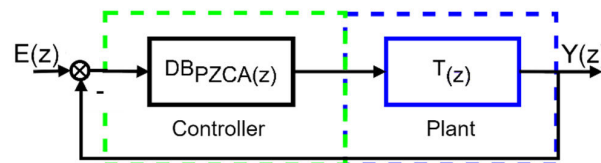

FIGURE 5. Discrete-time unity-feedback control system.

2) FACTORIZATION (POLYNOMIAL) DEADBEAT CONTROL APPROACH

Independent of the research methods of pole-zero cancellation, another line of research emerged based on the input-output approach. A prominent research work on the polynomial approach was the study pioneered by [15]. The author described the system's plant as a ratio of polynomials in the delay operator d. The author used the same description as in the PZCA in defining the reference input. This method provided an improvement from the PZCA, where the cancellation of the plant's poles lying outside the unit circle by the controller's zeros is avoided. This approach follows a similar path as the PZCA with some modifications. Considering the block diagram in Figure 5, the plant can be expressed in the form of compensable and non-compensable poles and zeros as:

$$T_{(z)} = \frac{B_{(z)}}{A_{(z)}} z^{-d} \quad (6)$$

The numerator and denominator are split into poles and zeros inside and outside the unit circle as:

$$\frac{B_{(z)}}{A_{(z)}} z^{-d} = \frac{B_{(z)}^+}{A_{(z)}^+} \frac{B_{(z)}^-}{A_{(z)}^-} z^{-d} \quad (7)$$

where polynomials $A_{(z)}^+$ and $B_{(z)}^+$ represent the poles and zeros inside the unit circle, respectively, and $A_{(z)}^-$ and $B_{(z)}^-$ represent the poles and zeros outside the unit circle, respectively. The desired closed-loop polynomials are chosen according to the expressions in (8) and (9):

$$N_{(z)} = B_{(z)} C_{1(z)} M_{(z)} z^{-d} \quad (8)$$

$$1 - N_{(z)} = A_{(z)} \left(1 - z^{-1}\right) Q_{(z)} \qquad (9)$$

where $C_{1(z)}$, $M_{(z)}$ and $Q_{(z)}$ are polynomials chosen to satisfy some conditions and z^{-d} represents the inherent delay in the plant of the system. Therefore, the desired controller can be expressed as:

$$\begin{aligned} DB_{f(z)} &= \frac{A_{(z)}^{+}}{B_{(z)}^{+}} \frac{A_{(z)}^{-}}{B_{(z)}^{-} \times z^{-d}} \times \frac{N_{(z)}}{1 - N_{(z)}} \\ &= \frac{A_{(z)}^{+} C_{1(z)} M_{(z)} z^{-d}}{\left(1 - z^{-1}\right) Q_{(z)}} \end{aligned} \qquad (10)$$

Turning polynomials $C_{1(z)}$ and $M_{(z)}$ are used to make the controller less aggressive and $Q_{(z)}$ is used to give the controller some degrees of freedom. This approach was adopted recently in [16], where the authors designed both the inner current loop and the outer voltage loop using this approach and applied the controllers to a single-phase inverter with one-carrier-period lag. The study achieved a good result and was unique because the authors used DBC in both loops. However, the research did not consider the influence of time delay and model parameter variation, which are critical and always challenging the system's stability. Undoubtedly, the PZCA and the factorization approach demonstrate good and finite settling time when handing discrete systems, but for sampled data, the issue of ripples at the inter-sampling point may pose a challenge. To address this issue, another kind of approach emerged, called the FRA, which is ripple-free at the inter-samples.

In a deadbeat control of discrete plants that originate from a continuous system, it is imperative to have a deadbeat control at and between the sampling instants. This approach is built on the idea of the previous method. Still, there is no zero cancellation of the plant transfer function either inside or outside the unit circle, and there are added constraints that increase the response time of the system. In [17], the author presented mathematical formulation and analysis on ripple-free deadbeat control (RFDBC) and stated that if $G_p \left(z^{-1}\right) = Q \left(z^{-1}\right)/P \left(z^{-1}\right)$ represents a sampled data transfer function, then output, input, $Q \left(z^{-1}\right)$ and $P \left(z^{-1}\right)$ are coprime polynomials with $P(0) \neq 0$ to assure causality. Also, if pure time delays are accounted by the leading zero coefficients in $\left(z^{-1}\right)$, then a ripple-free DBC is achieved by Equation 11:

$$DB_{rf} \left(z^{-1}\right) = \frac{P \left(z^{-1}\right)}{Q(1) - Q \left(z^{-1}\right)} \qquad (11)$$

This method was adopted in [16] to control a single-phase inverter with one-carrier-period lag, and the researchers employed two DB controllers: a current controller in the inner loop and a voltage controller in the outer loop. This study achieved a good result based on the lower total harmonic distortion (THD) obtained. However, the research did not consider time-delay compensation and the method adopted for the model mismatch was not clearly stated. Recently, in [18], the authors proposed a deadbeat controller design for single-phase active power filters based on forward-backward

discretization; this method reduced the parameter dependency of the deadbeat controller, which has always been questioned. This procedure offers high accuracy in modeling and, at the same time, simplicity in designing the deadbeat controller, according to the authors in [18]. However, the proposed discretization method has drawbacks on the time step size to ensure numerical stability. The authors [19] proposed a soft-deadbeat control for a multivariable three-phase voltage-source converter under variable grid voltage. Three filters were tested in this research work, which were the finite impulse response (FIR) and the first- and second-order infinite impulse response (IIR) filters. Good results were obtained from this research work. However, this research failed to clearly explain whether the deadbeat controller was applied in the entire system or to only part of the system.

3) STATE-VARIABLE DERIVATION (POLE PLACEMENT TECHNIQUE)

This class of deadbeat control's main idea is to prescribe a system where all closed-loop poles are placed at the origin without pole cancellation to achieve a finite settling time for the step input signal in *n* time-steps. Assuming a system to be controllable with state transition matrices *A* and *B*, it can be represented as in Equation 12:

$$x (k + 1) = Ax (k) + Bu (k) \qquad (12)$$

$$Y (k) = C^T x (k) \qquad (13)$$

The state-feedback control law as shown in Figure 6 has the form of:

$$u (k) = -K^T x (k) + K_w E (k) \qquad (14)$$

This law assumes that the state variables are available for feedback, and by substituting 14 into 12, we have:

$$x (k + 1) = \left(A - BK^T\right) x (k) + BK_w E (k) \qquad (15)$$

Equation 14 represents the deadbeat control law which reduces the problem of determining the feedback gain K^T, where the eigenvalues of $A - BK^T$ all lie at the origin of the unit circle. Bass-Gura or other pole placement techniques are possible. The pulse transfer function is obtained by combining the Z-transform of Equations 13 and 15 to have Equation 16.

$$\frac{Y_{(z)}}{E_{(Z)}} = C^T \left[[zI - A] + BK^T\right]^{-1} BK_W \qquad (16)$$

To obtain constant K_w, the steady-state gain of the closed-loop function of Equation 16 is set to unity. This method was adopted in [20], where the authors proposed a cost-effective deadbeat current controller for wind-energy inverter application with LCL filter. The study employed a state observer to compensate for the time delay, where a good result was reported from the THD recorded. However, the research did not explain how model parameter sensitivity was tackled. Additionally, the controller's settling time was poor: it was more than three samples, which was higher than the

system's order. In [21], the authors proposed a state-vector feedback gain for DBC of a GCI with LCL filter, where better attenuation of switching harmonics and damping was reported. However, the study did not consider the influence of time delay and model parameter variation, which is crucial in digital implementation.

In [22], the authors proposed a control scheme for pulse-width modulation (PWM) voltage-source distributed generation inverter with fast load-voltage regulation and effective mitigation of unbalanced voltage disturbances. The study employed a DB current controller in the inner loop and a hybrid voltage controller with a variable structure control element in the outer loop. An adaptive uncertainty observer was employed to compensate for time delay as well as parameter mismatch. However, the observer employed was sensitive to changes in system parameters, in addition to having inherent modeling error and a large prediction error [23]. In [24], the authors adopted the DB controller designed in [25] and proposed a control method to mitigate fast voltage disturbances. The study employed a PI voltage control in the outer loop. However, the results presented were more of the same. In [26], the authors proposed an advanced SVPWM-based predictive current controller for three-phase inverters in a distributed generation system with the L output filter. This study employed double sampling and updating techniques to mitigate the time delay in the system. The authors concluded that a small delay was necessary to keep the system more robust to parameter variation. However, there is a need to investigate this method using the LCL output filter. In [27], the authors proposed a calculation-delay tolerant-prediction current controller for three-phase inverters. The study employed a state-feedback design approach with a Luenberger prediction observer to mitigate the time delay. The authors believed that mitigating the time delay enhanced the system's immunity to model and parameter uncertainties. However, there is a need to further investigate the method with higher-order filters. In [28], the authors used this approach to control a three-phase Z-source grid-connected wind power generation. The authors used a DBC in the inner loop and a PI controller in the outer loop. However, this research failed to consider the issues of time delay and model parameter variation, which are critical for this type of controller. In [29], the authors used this approach to control a three-phase grid-connected inverter with near deadbeat response. Good online monitoring of the equivalent impedance and adaptive changing of the plant parameters were achieved in this research work. However, due to the estimation of the parameters and the effect of discretization, the deadbeat control response was not exactly achieved.

4) HYBRID DBC DESIGN APPROACH
Since DBC demonstrates challenges due to model and parameter variation, some researchers decided to use this controller in series or parallel (as a single controller) with another controller. The finite settling time of the DBC is retained, and the other controller, such as repetitive or PI controller, enhances
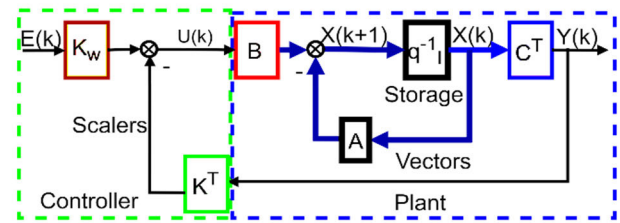
FIGURE 6. Block diagram of SVDA.

its robustness. This type of control approach is shown in Figure 7, where a deadbeat controller is cascaded with an integral controller. In this approach, new extended state and output equations are formed by defining an additional state variable. Assuming the system to be controllable with state transition matrices A and B, as in the previous method, the new extended equations can be represented as in 17 and 18:

$$\begin{bmatrix} X(k+1) \\ V(k+1) \end{bmatrix} = \begin{bmatrix} A & 0 \\ -C^T & 1 \end{bmatrix} \begin{bmatrix} x(k) \\ v(k) \end{bmatrix} + \begin{bmatrix} B \\ -C^TB \end{bmatrix} u(k)$$
$$+ \begin{bmatrix} 0 \\ 1 \end{bmatrix} E(k+1) \qquad (17)$$

$$Y(k) = \begin{bmatrix} C^T & 0 \end{bmatrix} \begin{bmatrix} x(k) \\ v(k) \end{bmatrix} \qquad (18)$$

Some researchers have adopted this approach; for example, in [30], the authors proposed a multi-loop DBC-repetitive and adaptive control for power converters with the LCL filter. Fast convergence with disturbance rejection was reported in this work, in addition to the possibility of adaptable control of the grid-side current. This achievement is not possible when implementing a single-loop control due to the plant's non-minimum-phase behavior. However, the additional loops used have cost and reliability implications. In [31], the authors presented a deadbeat repetitive current controller (RCC) in parallel with DBCC for grid-connected applications with the LCL filter. In this proposed control, the characteristic of fast dynamic-response tracking of the DBC was utilized, and the RCC made the steady-state error converge to zero gradually. According to the authors of this research, the proposed approach improved the quality of the feed-in grid current effectively. However, the study mentioned that a lead compensator should be used to compensate for the delay, but no such design was reported. Additionally, model parameter variation common to this controller was not considered.

5) ROBUST DEADBEAT CONTROL DESIGN APPROACH
The robustness of a controller is the controller's ability to exhibit excellent desired performance in the operations of both the nominal model of the system and any model contained within the set of models bounded by the specified range of model uncertainties [32], [33]. For a grid-connected inverter to have a robust control, it requires either an inner current control loop and an outer voltage control loop or an inner current control loop and an outer power control

loop, as the case may be. Such controllers in a deadbeat setting can be implemented by having pre-filters before the main controllers [34] or by having a pre-filter controller and another parallel controller (bridged-T controller). This type of controller is used in a control system for both setpoint control and disturbance rejection.

To achieve robustness, the block diagram of Figure 5 in Subsection B was modified into those in Figures 8(a) and (b), which are the DBCs with pre-filter and bridge-T controller, respectively. For the deadbeat with pre-filter, as shown in Figure 8a, $DB_{pf(Z)}$ is the pre-filter and $DB_{mc(Z)}$ is the main controller. $DB_{mc(Z)}$ can be represented by Equation 19 using the same description of the polynomial in Equation 10 and the pre-filter controller is represented by Equation 20, assuming the plant is a minimum-phase system:

$$DB_{mc(Z)} = \frac{1 - \left(1 - z^{-1}\right) A_{(z)} C_{D(z)}}{\left(1 - z^{-1}\right) B_{(z)} C_{D(z)}} \qquad (19)$$

$$DB_{pf(Z)} = \frac{B_{(z)} C_{w(z)} / B_{(1)} C_{w(1)}}{1 - \left(1 - z^{-1}\right) A_{(z)} C_{D(z)}} \qquad (20)$$

where $C_{W(z)}$ is a polynomial with which the gain can be used to handle the control variable constraints, expressed in the form of $C_{w0} + C_{w1}z^{-1} + C_{w2}z^{-2} + C_{w3}z^{-3} + \ldots$, and $C_{D(z)}$ is a polynomial that can be chosen arbitrarily to satisfy the control variable constraints. If the plant is a non-minimum-phase system, the two controllers can be re-written as in Equations 21 and 22.

$$DB_{mcn(Z)} = \frac{H_{(z)}}{\left(1 - z^{-1}\right) B_{(z)}^+ C_{D(z)}} \qquad (21)$$

$$DB_{pfn(Z)} = \frac{B_{(z)} / B_{(1)}}{1 - \left(1 - z^{-1}\right) A_{(z)} C_{D(z)}} \qquad (22)$$

The polynomial $H_{(z)}$ can be obtained using the relationship of $B_{(z)}^- H_{(z)} = 1 - \left(1 - z^{-1}\right) A_{(z)} C_{D(z)}$ and it should be noted that the degree of this polynomial has to correspond to the degree of the left-hand side of the expression.

Additionally, the bridged-T controller's configuration lends itself naturally to a robust control design in a deadbeat setting [6]. It is worth noting that the bridged-T controller fits in the general form of a two-degrees-of-freedom controller, and as such, it has the potential of robust performance, as demonstrated in [35]. Figure 8b shows a closed-loop control system that includes the bridged-T controller. The plant is represented by $T_{(z)}$ and the controller consists of three controllers: $DB_{pf(z)}$, $DB_{mc(z)}$ and $DB_{oc(z)}$. $R_{(z)}$ is the input, which is the reference to be tracked, and $D_{(k)}$ is the disturbance, which represents the model mismatch. $DB_{oc(z)}$ is an open-loop compensator, which is designed in such a way that $DB_{oc(z)}T_{(z)}$ gives a suitable response to reference input signal $R_{(z)}$. The design of the $DB_{oc(z)}$ controller involves the cancellation of the undesirable parts of plant transfer function $T_{(z)}$ such that the plant becomes stable. If the system is targeted to achieve a deadbeat response to the step input,

then $DB_{oc(z)}$ is chosen as:

$$DB_{oc(z)} = \frac{1}{T_{(z)}} \times \frac{P_{(z)}}{Z^m} \qquad (23)$$

where $P_{(z)}$ is chosen to include the zeros of the plant transfer function outside the unit circle so that the controller will be stable. Similar criteria were presented in [36]. The $DB_{pf(z)}$ controller gives a desired control system model that is related to $DB_{oc(z)}$ as:

$$DB_{pf(z)} = DB_{oc(z)} \times T_{(z)} = \frac{P_{(z)}}{Z^m} \qquad (24)$$

The last controller is feedback compensator $DB_{mc(z)}$, whose function is to correct the non-zero errors. However, if ideal conditions are assumed, the choice of the earlier two controllers results in zero error and therefore $DB_{mc(z)}$ is not needed. However, under practical considerations, the $DB_{mc(z)}$ controller is the only controller that directly influences the close-loop system's stability and, as such, it is required for robustness and disturbance rejection. As reported in [6], the design of $DB_{mc(Z)}$ does not depend on other controllers ($DB_{pf(z)}$ and $DB_{oc(z)}$). As such, it is treated independently without reference to the deadbeat control or the bridged-T controller. For reduction of error, $DB_{mc(Z)}$ is chosen to minimize the weighted sensitivity function [6] as:

$$S_{(z)} = \frac{1}{1 + T_{(z)} DB_{mc(z)}} f_{(z)} \qquad (25)$$

where $f_{(z)}$ is a frequency-weighting transfer function, which takes into account the frequency content of the disturbances and modeling errors affecting the system. For stability margin improvement, $DB_{mc(z)}$ is chosen to minimize the weighted complementary sensitivity as in Equation 26:

$$E_{(z)} = \frac{T_{(z)} \times DB_{mc(z)}}{1 + \times DB_{mc(z)}} f_{(z)} \qquad (26)$$

The competing objectives of minimizing both $S_{(z)}$ and $E_{(z)}$ can be combined in a single performance index to be optimized. The advantage of the bridged-T controller is that nominal deadbeat response is achieved first by the design of blocks $DB_{oc(z)}$ and $DB_{pf(z)}$ outside the loop. Then, independent of the deadbeat design, robustness is achieved separately by the design of feedback compensator $DB_{mc(z)}$.

Research works that adopted this approach include the research in [37], where the authors presented an improved deadbeat control with a repetitive plug-in controller. The study employed a repetitive controller in series with a robust DBC based on a controller with a pre-filter approach for grid current tracking (as a single controller). The controllers were combined to provide rejection of periodic disturbances, while keeping excellent dynamic response. A linear-phase-lead compensator was used to compensate for time delay.

According to the authors, the proposed approach improved the quality of the feed-in grid current significantly. However, the method employed to handle parameter variation was not intuitively explained. In [38], the study discussed a
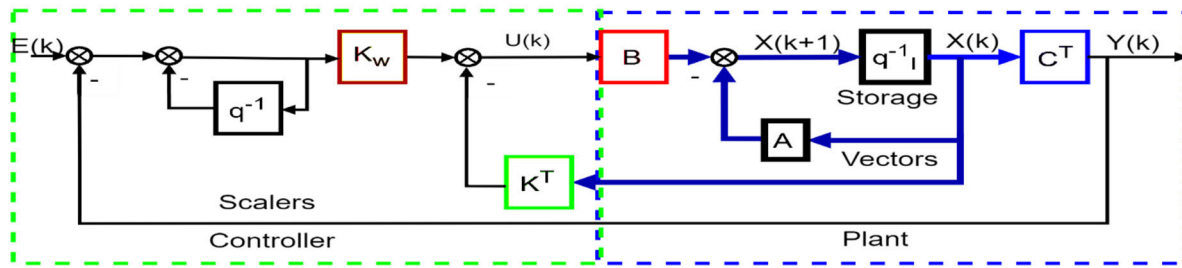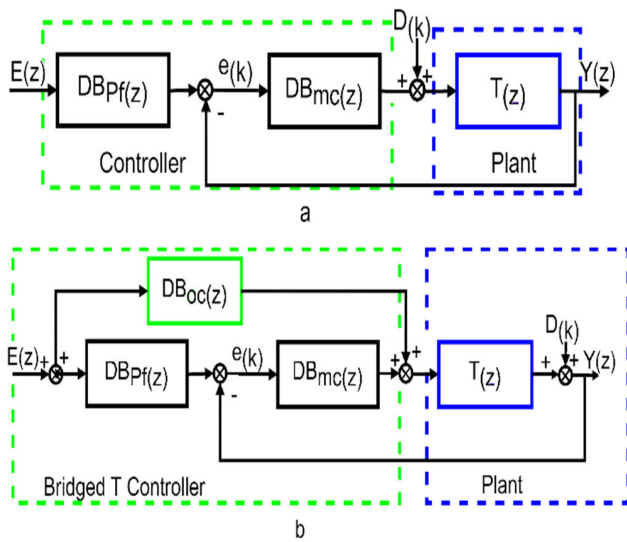
FIGURE 7. Block diagram of HBDA.

FIGURE 8. Closed-loop control system with pre-filter and bridged-T controller. (a) Controller with pre-filter. (b) Controller with T-bridge.

synchronous-reference-frame robust predictive current control, where DBC was used in the inner loop and a PI controller was used in the outer loop. The authors employed a controller approach with a pre-filter with a diagonal Luenberger observer to compensate for time delay. The realized controller enhanced the stability limits against control delays and inductance variations. There is room for better results by adopting better time-delay compensation techniques, as suggested by [2]. In [39], the authors extended the previous work presented in [38] by using an LCL filter instead of the L filter and modeled the system with an arbitrary control delay. However, the observer employed had inherent modeling error and large prediction error [23].

In [40], the authors presented a robust predictive dual-loop control strategy for a grid-connected photovoltaic (PV) generation system. The study employed DBC and PI control in the inner and outer loops, respectively. The authors claimed that time delay and inductance variation were taken care of, but the method employed was not clearly explained. In [34], the authors extended the scope of a previously presented work by adding an extra power feed-forward loop with reactive current detection to compensate for time delay and

grid-voltage prediction to compensate for parameter mismatch. This work recorded good results in terms of time delay and THD. However, there is room for further reducing the time delay. In [41], the authors presented a robust current control with harmonics compensation. Five different controllers were employed in this work: active damping controller, inner current controller, outer voltage controller, grid current controller and harmonics prediction controller. A Luenberger estimator was employed to handle parameter variation, but time delay was ignored in this research. Additionally, key performance parameters, such as THD at the inverter's output, were not mentioned to guide future research.

Recently, in [42], the authors presented a fast, robust pulse-width-modulation (PWM)-based DBC. The influence of filter inductance variation was analyzed and the deviation coefficient of the system critical stability was found to increase with an increase in the equivalent resistance and an increase in the sampling frequency. The authors claimed that time delay was compensated using the fast, robust PWM but the method sampled the signal only three times and updated it only once. Therefore, a one-period delay still existed in the control loop. Additionally, the issues of model and parameter variation were not intuitively discussed in this work.

6) OTHER DESIGN APPROACHES
a: N-STEPS-AHEAD PREDICTION CONTROL
As earlier explained in Section I, deadbeat and N-steps-ahead controls were researched separately in the past, but the two ideas were later merged and called DBC [6]. However, some researchers still refer to their DBC approach as the N-steps-ahead control in recent times [18]. The fundamental idea behind the N-steps-ahead control is to determine the control signal required to force the output of a system to the desired level in N time-steps. Therefore, this method can form any form of the approaches earlier discussed in this section. As such, the present paper sought to bring to the reader's notice that such nomenclature still exists in the body of knowledge. We chose to classify all research on DBC that did not mention the approaches adopted, or cannot be presumed by us, as the N-steps-ahead prediction control.

N-steps-ahead prediction refers to the number of predicted steps the controller is expected to make for the output to reach

a finite stage. This technique is accomplished by subtracting the denominator (poles) dynamics and algebraically cancelling the numerator (zeros) dynamics [43]. The control law is developed in the time domain using a difference equation with the plant, described as:

$$
\begin{aligned}
y^* (n+k) &+ a_{k-1} y^* (n+k-1) + \ldots + a_1 y^* (n+1) \\
&+ a_0 y^* (n) = b_{n+k-1} u (n+k-1) + b_{n+k-2} u (n+k-2) \\
&+ \ldots + b_0 u (n)
\end{aligned} \tag{27}
$$

where $y^* (n+k)$ is the output at the next time-step, of which the desired value is $y^* (n+k)$, and the present control signal is $u (n+k-1)$. Therefore, as the desired output at the next step is $y^* (n+k)$, the present output is $y^* (n+k-1)$, and from all the previous inputs and outputs, it is possible to solve for the present control signal $u (n+k-1)$ as:

$$
\begin{aligned}
u &(n+k-1) \\
&= -\frac{1}{b_{n+k-1}} \left(b_{n+k-2} u (n+k-2) \right. \\
&\quad + \ldots + b_0 u (n) - y^* (n+k) - a_{k-1} y^* (n+k-1) \\
&\quad \left. - \ldots - a_1 y^* (n+1) - a_0 y^* (n) \right)
\end{aligned} \tag{28}
$$

Equation 28 represents the N-steps-ahead controller. This technique has been adopted more than any other technique in the literature. In [44], the authors proposed a vector-current-controlled voltage-source converter using the one-step-ahead (OSA) approach. The study employed the Smith predictor to mitigate time delay. However, key performance indicators were not mentioned to ascertain the output's quality, such as the minimum time delay achieved and the THD. Additionally, this research did not consider the issue of model parameter variation in the design, which is critical. In [12], the authors proposed a robust predictive current control for three-phase grid-connected inverters; the study employed a two-steps-ahead prediction approach with a Luenberger observer to compensate for time delay. Consequently, the researchers believed that their research improved the tolerance to parameter variation from the previous research. However, the method adopted to support this claim was not stated. In [45], the authors reviewed and evaluated some current control methods and proposed a simple DBC based on one-step-ahead prediction. The study focused on improving the system's robustness to model and parameter mismatch. The authors believed that by increasing the damping resistor's value, the system gets immune to those mismatches. However, the study failed to employ any time-delay compensation techniques, which is a challenging factor in digital implementation. Additionally, increasing the resistance is at the expense of an increase in power loss, which is highly undesirable. In [46], the authors considered a deadbeat control based on current prediction calibration for grid-connected converters under unbalanced grid voltage. The study employed a DBC using one-step-ahead prediction in the inner loop and PI control in the outer loop. The study mentioned time delay and model and parameter variation issues, but the method adopted to mitigate both the time delay and the mismatch was unclear. In [47],

the author proposed a conceptual design to suppress low- and high-frequency instabilities and grid inductances in a distributed inverter. The study employed an OSA controller in the inner loop and a PI controller in the outer loop. An adaptive disturbance observer was employed to mitigate time delay and model parameter mismatch. This study reported good controller tracking with a deadbeat response. However, an observer may be sensitive to changes in the system parameters in addition to having inherent modeling error and a large prediction error [23]. In [48], the authors proposed a robust line-voltage sensorless control and the synchronization of the DB controller using the two-steps-ahead approach. Deadbeat current controller and PI controller were employed in the inner and outer loops, respectively, and a natural observer was used to compensate for time delay and model parameter mismatch. A good result was reported from this study. However, the observer could not compensate the time delay reasonably, as the value of the delay in the control loop was up to $1ms$. There is a need to test this method with a better compensation method, as suggested by [2]. In [49], the authors proposed a robust tracking of a three-phase DC-AC inverter for uninterruptible power supply (UPS) applications. The study employed the OSA approach with linear-matrix-inequality-based optimization, wherein a good THD value was recorded.

However, there is a need to expand this research to grid-connected applications. In [50], the authors presented the analysis and characterization of a large-bandwidth triple-loop controller for grid-connected inverters. This study employed two DB current controllers and a PI voltage controller, where good performance characteristics were recorded. However, how time delay and model parameter variation were handled was not clearly explained; nevertheless, the three-loop controller employed increased the system's complexity, cost and lack of reliability [51]. In [52], the authors used the OSA approach to present an improved DBC strategy based on interpolation prediction and online inductance identification. The study applied a DBC in the inner loop and a PI controller in the outer loop. At the same time, a Newton prediction algorithm was proposed for time-delay compensation, and an online inductance parameter identification algorithm was proposed to take care of the model and parameter variation present. However, the output of this research was characterized by high THD of output current at lower input power, which can be improved by adopting an LCL filter instead of an L filter. In [53], the authors researched an improved deadbeat current control algorithm using a prediction algorithm. However, the method adopted in compensating for time delay and model parameter variation was not clearly explained.

In [54], the authors presented an evaluation of a DB current controller for a grid-connected application. Both OSA and two-step-ahead (TSA) approaches were used for the DBC design, and the proportional gain reduction approach and the Smith predictor approach were compared for their ability to compensate for the time delay. Additionally, this study employed voltage prediction to take care of the variation in

the model and the parameters. However, key performance indicators, such as the minimum time delay achieved and the THD recorded, were not clearly mentioned to guide further research. In [55], the authors conducted a comparative review of predictive current control techniques applied to single-phase grid-connected inverters and presented a comparative analysis of the two most prominent ones: the DBC and the model predictive control (MPC). The comparison highlighted the main differences and clarified the confusion as to whether they belong to the same class. However, the analysis did not give a clear picture of the types of DBC. Therefore, there is a need to investigate this comparison further. In [11], the authors proposed a unified startup strategy for modular multi-level converters with deadbeat predictive current control. This study took up the main challenge of modular multi-level converters, which is the pre-charge of all submodule (SM) capacitors to their nominal voltage value during the startup process. Using the deadbeat strategy, the authors believed that a fast pre-charge for all SM capacitors from either the AC- or DC-side main voltage without any inrush current was effectively realized. However, this method needs to be investigated further using a higher-order output filter to achieve a better output current. In [56], the authors proposed a multivariable deadbeat control of power electronics converters with fast dynamic response and fixed switching frequency. This research work employed the DBC for the entire system, therefore accelerating the time response not only for the current loops but also for the voltage loops. Good results were obtained based on the simulation in this research. However, there is a need to further investigate this method using a higher-order output filter.

b: UNCLASSIFIED DBC

A deadbeat control discussion will not be complete without mentioning that some research attempted to use known conventional controllers to achieve a deadbeat response at the system's output. It is worth noting that such controllers still retain their properties and their controller name, but the researchers used the word deadbeat to describe how fast their controller's response is. Discrete controllers, such as PI and sliding mode [57], have been used by some researchers and they named the responses as deadbeats. Such studies include the research works in [9], [44], [58], [59] and [60], where the overall closed-loop poles of the system adopting this approach were placed at the origin using simple mathematics.

In [44], the authors presented a vector-current-controlled voltage-source converter adopting this design approach, where a Smith predictor was employed to compensate for time delay, and a back-calculation algorithm was used to handle the issue of the integrator windup. In this work, good performance in terms of dynamic vector limiting leads to a balance between fast response and independent current control. However, during large transients, the demanded reference voltage of the DB controller may not be deadbeat. In [58], the authors presented a hybrid control method for three-phase grid-connected inverters with high-quality

power. The study employed a digital PI control with space vector pulse-width modulation (SVPWM) and dual-time sampling and updating techniques to handle the control loop's time delay. According to the authors, the proposed method effectively improved the quality of the output current. However, there is a need to investigate this approach with the LCL filter. In [59], the authors presented a PI-based SVPWM controller for a three-phase PV system that mimicked a DBC in the synchronous reference frame. As reported by the authors, convenient active and reactive power decoupling and insensitive controller in parameter variation were realized. However, this research failed to account for the delay present in the control loop. In [9], the authors proposed a synchronous-reference-frame PI controller with a deadbeat response. The proposed controller introduced a noticeable improvement in transient and steady-state responses to disturbances in the control loop.

In [61], the authors investigated the performance of three deadbeat predictive controllers for a three-level neutral-point-clamped inverter, and the investigation was based on computational burden, current THD, voltage balancing, average switching frequency and dynamic response. Good results were achieved from the proposed improved method. However, there is a need to investigate this method further using other types of filters. Recently, in [62], the authors presented an improved deadbeat control strategy based on repetitive prediction against grid frequency fluctuation for an active power filter. The research work aimed at improving the harmonic compensation performance of the active filter in a distribution network. The authors believed strongly that their proposed method had an acceptable steady-steady response to grid frequency variation and a satisfactory dynamic response to the change in the load current. However, based on the zero-pole distribution plot in the research work, the closed-loop poles were not placed even close to the origin but adequately contained within the unit circle. Therefore, the use of the term "deadbeat" could be misleading in this case. Additionally, in [62], the authors proposed a deadbeat current controller for a bidirectional dual-active-bridge converter using the enhanced single-phase shift (ESPS) modulation method by exploiting pulse width as an extra control variable besides the phase-shift ratio. Parameter robustness was analyzed by mathematical derivation, and the online auto-tuning method for the inductance was presented. This method was simple to design and implement, according to the authors. However, the approach adopted cannot be clearly understood.

c: CONSTRAINED DBC

A DBC increases the step response speed of a system by manipulating input variables in two ways. The first is to allow the large signal (positive) to proportionally drive system response very fast to obtain the desired initially constant value. A delayed smaller step signal (negative) follows, which targets to cancel the remainder of the transient response from the large step signal [54]. Nevertheless, a large positive signal (control signal) can be too large to be scaled down. In such

circumstances, the deadbeat controllers discussed earlier may be referred to as constrained DBCs. However, this constraining has the effect of increasing the degree of the controller and, consequently, increasing the overall degree of the closed-loop system, which also translates into increased time for the system to settle and some overshoot, to mention but a few. In the next section, a comparison of some control strategies will be presented.

III. COMPARISON OF SOME CONTROL STRATEGIES

For comparison, a grid-connected inverter with LCL filter and active damping as proposed in [63] was adopted. The control loop of the inverter adopting the grid-side current control with a feedback of the capacitor current for the active damping LCL filter is shown in Figure 9, where P_L represents the third-order filter and K_{pwm} represents the gain of the full-bridge three-phase inverter [64], which can be approximated by Equation 29:

$$K_{pwm} = \frac{U_{dc}}{2} \qquad (29)$$

The loop gain of the control system from Figure 9 can be written from U_c to I_g as in Equation 30:

$$T_{(s)} = \frac{I_g}{U_c} = \frac{K_{pwm}}{s^3 \left[L_i L_g' C_f\right] + s^2 K_{pwm} k_d C_f L_g' + s \left[L_i + L_g'\right]} \qquad (30)$$

where:

$$L_g' = L_g + L_{gs}$$

Putting the open-loop control of the output transfer function into the standard normalized quadratic form [63], the damping ratio ζ can be given by:

$$\zeta = \frac{k_d K_{pwm}}{2} \times \sqrt{\frac{\left(L_g + L_{gs}\right) C_f}{L_i \left(L_i + L_g + L_{gs}\right)}} \qquad (31)$$

Based on Equation 31, the higher the damping factor ζ, the better is the damping effect on the system. However, a very high value for ζ will reduce the overall stability margin of the system. Thus, a better tradeoff can be achieved with $\zeta = 0.707$ [63], [64] and k_d can be simply calculated using Equation 31. The parameters used in [63] were adopted in this research, as shown in Table 2. Finally, using the inverter parameters listed in Table 2 and using different values of k_d, the Bode plot in Figure 10 justified the selection of damping constant k_d. The curve flattened as the value of k_d increased.

To compare some of the control approaches presented in the previous section, we shall consider the output equation in 30. The grid voltage can be assumed to be an ideal voltage source, and for frequencies other than the fundamental, the grid side can be considered a short circuit [65]. Therefore, the transfer function from Equation 30 can be expressed based on Table 2 as in Equation 32, which serves as the plant to be controlled:

$$T_{(s)} = \frac{340}{2.006e^{-11}s^3 + 4.702e^{-7}s^2 + 0.005512s} \qquad (32)$$

Using the zero-order hold (ZOH) method of discretization and using a sampling frequency of 10 kHz, the discrete form of the transfer function is as in Equation 33:

$$T_{(z)} = \frac{1.5385\,(z + 1.976)\,(z + 0.1526)}{(z - 1)\,(z^2 - 0.2404z + 0.09597)} \qquad (33)$$

It is obvious from the zero-pole gain (zpk) in Equation 33 that the system has one zero lying outside the unit circle and one pole lying on the unit cycle. Therefore, there is a need to design a discrete controller that will pull the pole to lie inside the circle. Note that the deadbeat controller's design procedures are expressed in d-operator (z^{-1}), as discussed in Section II; therefore, by dividing the zpk by z, Equation 33 can be expressed as in Equation 34. Next, we designed a controller based on the formulas discussed in the previous section.

$$T_{(z)} = \frac{1.5385z^{-1}\left(1 + 1.976z^{-1}\right)\left(1 + 0.1526z^{-1}\right)}{\left(1 - z^{-1}\right)\left(1 - 0.2404z^{-1} + 0.09597z^{-2}\right)} \qquad (34)$$
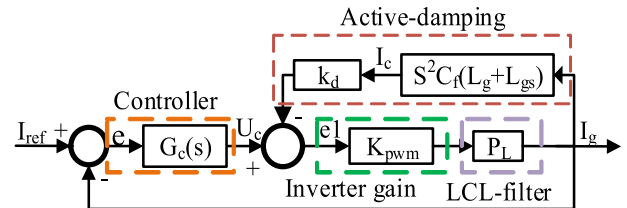
FIGURE 9. Block diagram of grid-side current control with active damping.
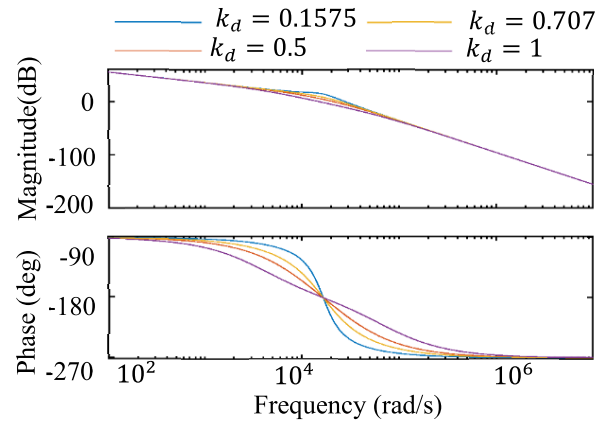
FIGURE 10. Bode plot with different damping factors.

A. POLE-ZERO CANCELLATION (PZC) APPROACH

Using the discretized zpk from Equation 34, the turning polynomial was obtained as:

$$m_k z^{-k} = 0.33602z^{-2}, \quad Q_{(z)} = 1 + z^{-1} + 0.6639z^{-2}$$

Therefore, the controller was obtained, as presented in Equation 35:

$$DB_{p(z)} = \frac{0.2184z^{-1}\left(1 - 0.2404z^{-1} + 0.09597z^{-2}\right)}{\left(1 + 0.1526z^{-1}\right)\left(1 + z^{-1} + 0.6639z^{-2}\right)} \qquad (35)$$

TABLE 2. Inverter parameters.

INVERTER PARAMETERS	
Rated power, p	80 kW
Switching frequency, f_s	10 kHz
Sampling frequency, f_{sw}	10 kHz
DC-link voltage, U_{dc}	680 V
Grid impedance, L_{gs}	0.012 mH
Inverter-side inductor, L_i	4.58 mH
Grid-side inductor, L_g	0.92 mH
Grid nominal voltage, U_g	230 V_{rms}
Filter capacitance, C_f	4.7 μF
Damping factor of capacitor current, k_d	0.3157
Damping ratio, ζ	0.707

A desired closed-loop pulse transfer function was given by:

$$N_{(z)} = A^+_{(z)} m_k z^{-k} = 0.33602 z^{-2} \left(1 + 1.976 z^{-1}\right)$$

and presented as in Equation 36:

$$N_{(z)} = \frac{0.33602 \, (z + 1.976)}{z^3} \tag{36}$$

The step and Nyquist plots are shown in Subplots (a) and (b), respectively, in Figure 11a. As evident from the plots, the system settled at 3 sampling periods with no overshoot, and from the Nyquist plot, there was no encirclement of the critical point, which indicated that the closed-loop system was stable.

B. FACTORIZATION (POLYNOMIAL) DEADBEAT CONTROL APPROACH

Using the discretized zpk in Equation 34, the turning polynomial was obtained as $M(z) = 0.2915 z^{-1}$, $C_{1(z)} = 1$ and $Q_{(z)} = 1 + 0.7085 z^{-1} + 0.08789 z^{-2}$. Therefore, the controller was obtained based on Equation 10, as presented in Equation 37:

$$DB_{f(z)} = \frac{0.18949 \left(z^2 - 0.2404 z + 0.09597\right)}{(z + 0.1516) \left(z^2 + 0.8484 z + 0.5798\right)} \tag{37}$$

The desired closed-loop pulse transfer function was obtained as in Equation 38:

$$F_{(z)} = \frac{0.2915 \, (z + 1.976) \, (z + 0.1526)}{z^4} \tag{38}$$

The step and Nyquist plots of this technique are shown in Subplots (c) and (d), respectively, in Figure 11b. As evident from the plots, the system settled at 4 sampling periods with no overshoot, and from the Nyquist plot, there was no encirclement of the critical point, which indicated that the closed-loop system was stable.

C. STATE-VARIABLE DERIVATION (POLE PLACEMENT TECHNIQUE)

The pulse transfer function in Equation 34 was converted into the state-space in control canonical form as:

$$A = \begin{bmatrix} 0 & 1 & 0 \\ 0 & 0 & 1 \\ 0.0960 & -0.3364 & 1.24 \end{bmatrix} B = \begin{bmatrix} 0 \\ 0 \\ 1 \end{bmatrix}$$

$$C = \begin{bmatrix} 0.4638 & 3.275 & 1.5380 \end{bmatrix}$$

Let K^T represent the constant required to place the pole at the origin and the characteristic polynomial be represented by X_C, as in Equation 39:

$$K^T = \begin{bmatrix} k1 & k2 & k3 \end{bmatrix}$$
$$X_C = \begin{bmatrix} [z * I - A] + B * K^T \end{bmatrix} \tag{39}$$

Matrix K^T was obtained by comparing Equation 39 with the desired polynomial at the origin; therefore, matrix K^T was obtained as:

$$K^T = \begin{bmatrix} 0.09597 & -0.3364 & 1.24 \end{bmatrix}$$

K_W was obtained by solving Equation 16 for unity gain:

$$K_W = 0.1895$$

Considering the signal from the input to the output as shown in Figure 6, the overall transfer function can be obtained using Equation 40:

$$\frac{Y_{(z)}}{E_{(Z)}} = C^T \left[zI - A\right] + BK^T \Big]^{-1} BK_W \tag{40}$$

Therefore, the closed-loop matrices became:

$$\hat{A} = \begin{bmatrix} 0 & 1 & 0 \\ 0 & 0 & 1 \\ 0 & 0 & 0 \end{bmatrix}, \quad \hat{B} = \begin{bmatrix} 0 \\ 0 \\ 0.1895. \end{bmatrix}$$

Based on the new closed-loop matrices, the deadbeat controller and the closed-loop pulse transfer function were obtained as in Equations 41 and 42, and the step and Nyquist plots are shown in Subplots (e) and (f), respectively, in Figure 11b. As evident from the plots, the system settled at 3 sampling periods with no overshoot, and from the Nyquist plot, there was no encirclement of the critical point, which indicated that the closed-loop system was stable.

$$DB_{s(z)} = \frac{0.1895 \, (z - 1) \, (z^2 - 0.2404 z + 0.09597)}{z^3} \tag{41}$$

$$\frac{Y(z)}{E(z)} = \frac{0.29145 \, (z + 1.976) \, (z + 0.1526)}{z^3} \tag{42}$$

D. HYBRID DBC USING STATE-SPACE DESIGN APPROACH

To obtain a deadbeat control with integration of the control error, we constructed a new extended set of state and output matrices from the state matrices in method C with an additional variable called v, as described in Equations 17 and 18, from which K^T and K_W were obtained. The substituted new matrices were given as:

TABLE 3. Summary of simplified controllers, control laws and their output.

S/No.	Method	Controllers
1	PZCA	
	Inner control law	$U(k) = 0.2184N(k-1) - 0.05251N(k-2) + 0.02096N(k-3) - 1.153U(k-1) - 0.8166U(k-2) - 0.1013U(k-3)$
	Output difference equation	$Y(k) = 0.336E(k-2) + 0.664E(k-3)$
2	FRA	
	Inner control law	$U(k) = 0.1895N(k-1) - 0.04556N(k-2) + 0.01819N(k-3) - U(k-1) - 0.7087U(k-2) - 0.08797U(k-3)$
	Output difference equation	$Y(k) = 0.2915E(k-1) + 0.6204E(k-2) + 0.08798E(k-3)$
3	SVDA	
	Inner control law	$U(k) = 0.1895N(k) - 0.235N(k-1) + 0.06375N[(k-2) - 0.01819N(k-3)$
	Output difference equation	$Y(k) = 0.2915E[(k-1)] + 0.6206E[(k-2)] + 0.08789E[(k-3)]$
4	HBDA	
	Inner control law	$U(k) = 0.1895N(k+1) - 0.0235N(k) + 0.06375N(k-1) - 0.01819N(k-2) - 0.7085U(k-1) - 0.08792U(k-2)$
	Output difference equation	$Y(k) = 0.2915E(k-1) + 0.6206E(k-2) + 0.08789E(k-3)$
5	RCA	
	Inner control law	$U(k) = 0.6656N(k) - 0.5701N(k-1) + 0.1625N(k-2) - 0.03935N(k-3) - 0.3686U(k-1) + 1.183U(k-2) + 0.1856U(k-3)$
	Outer control law	$E(k) = 0.1301N(k) + 0.277N(k-1) + 0.03924N(k-2) + 0.7037U(k-1) - 0.1929U(k-2) + 0.04283U(k-3)$
	Output difference equation	$Y(k) = 0.1343E(k-1) + 0.489E(k-2) + 0.3373E(k-3) - 0.2523E(k-4) - 0.094E(k-5) - 0.007523E(k-6) + 0.3437Y(k-1) + 0.06038Y(k-2) - 0.02663Y(k-3) + 0.01542Y(k-4)$

$\tilde{A} = \begin{bmatrix} A & 0 \\ -C^T A & 1 \end{bmatrix}$, which is an $(n+1) \times (n+1)$ matrix,

$\tilde{A} = \begin{bmatrix} 0 & 1 & 0 & 0 \\ 0 & 0 & 1 & 0 \\ 0.09597 & -0.3364 & 1.24 & 0 \\ -0.1476 & 0.0536 & -5.1821 & 1 \end{bmatrix}$,

$\tilde{B} = \begin{bmatrix} B \\ -C^T B \end{bmatrix}$, $\quad \tilde{B} = \begin{bmatrix} 0 \\ 1 \\ -1.5380 \end{bmatrix}$, $(n+1) \times 1$ vector,

$\tilde{K} = \begin{bmatrix} K^T & -K_W \end{bmatrix}$,

$\tilde{K} = \begin{bmatrix} 0 & 0 & 0 & 1 \end{bmatrix} \begin{bmatrix} Q_c^{-1} \tilde{A}^4 \end{bmatrix}$ (43)

where Q_c is a controllability matrix.

$\tilde{K} = \begin{bmatrix} 0.09597 & -0.2485 & 1.9485 & -0.1895 \end{bmatrix}$

Therefore,

$K^T = \begin{bmatrix} 0.09597 & -0.2485 & 1.9485 \end{bmatrix}$

$K_W = 0.1895$, and the deadbeat controller was obtained as in Equation 44:

$DB_{hb=} \dfrac{0.1895z^3 - 0.235z^2 + 0.06375z - 0.01819}{z^2 + 0.7085z + 0.08792}$ (44)

The closed-loop reference transfer function was obtained from Equation 45:

$$FT = C^T \left(zI - G + BK^T\right)^{-1} BK_W z$$

$$FT = \frac{0.29145\,(z + 1.976)\,(z + 0.1526)}{(z + 0.5481)\,(z + 0.1604)} \quad (45)$$

The overall feedback transfer function from the input to the output is given by Equation 46, and the step and Nyquist plots are shown in Subplots (g) and (h), respectively, in Figure 11b. As evident from the plots, the system settled at 3 sampling periods with no overshoot, and from the Nyquist plot, there was no encirclement of the critical point, which indicated that the closed-loop system was stable.

$$\frac{Y_{(z)}}{E_{(Z)}} = \frac{C^T \left(z*I - G + BK^T\right)^{-1} BK_W z}{(z-1)\left(C^T \left(z*I - G + BK^T\right)^{-1} BK_W z\right)}$$

$$\frac{Y_{(z)}}{E_{(Z)}} = \frac{0.29145\,(z + 1.976)\,(z + 0.1526)}{z^3} \quad (46)$$

E. ROBUST DEADBEAT CONTROL DESIGN APPROACH

Since the inverter plant had zeros outside the unit circle, the formulas for the inner- and outer-loop deadbeat controllers in Equations 21 and 22 are used. These equations split
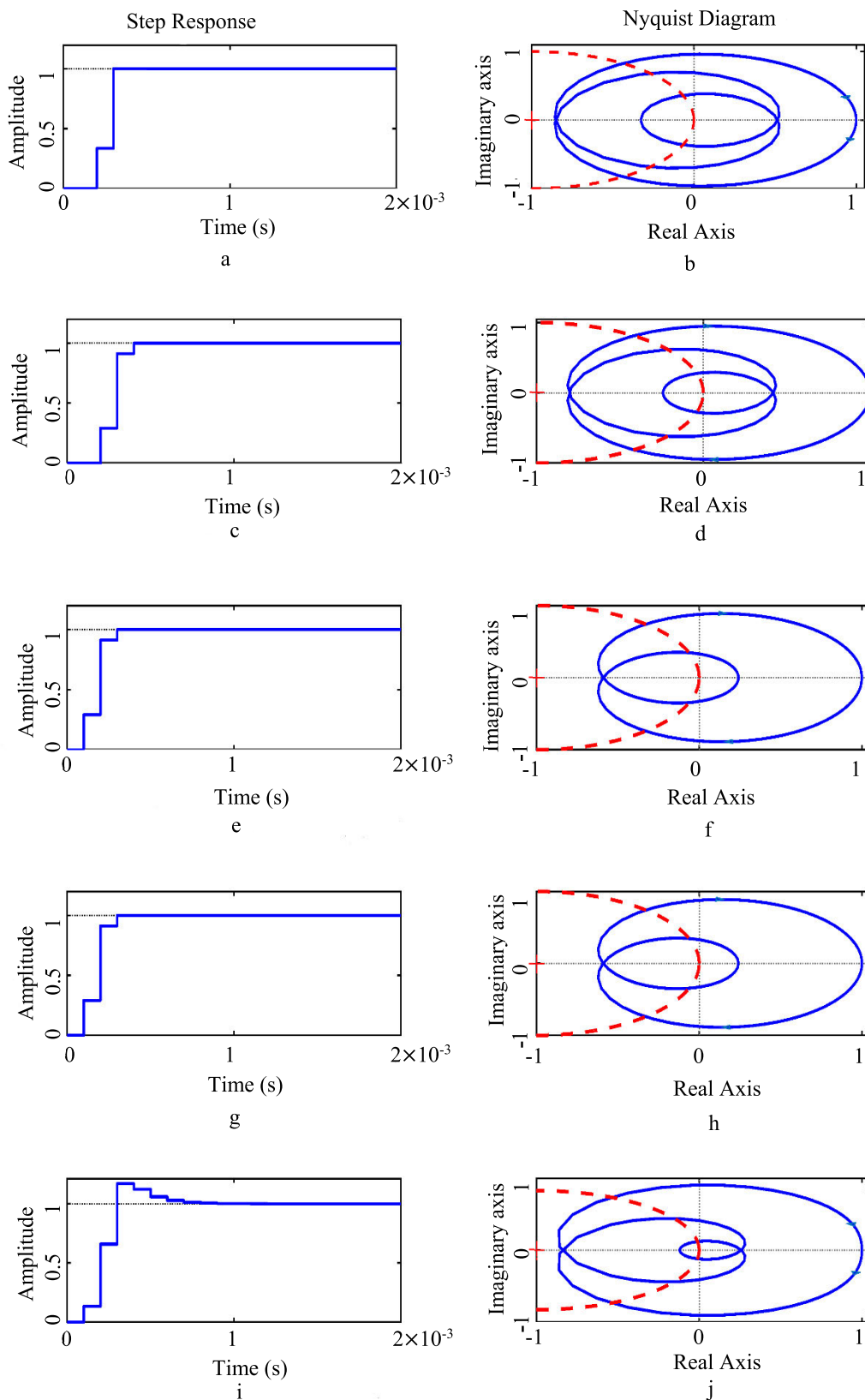
FIGURE 11. Step and Nyquist plots for (a,b) PZCA, (c,d) FRA, (e,f) SVDA, (g,h) HBDA and (i,j) RCA at steady state.
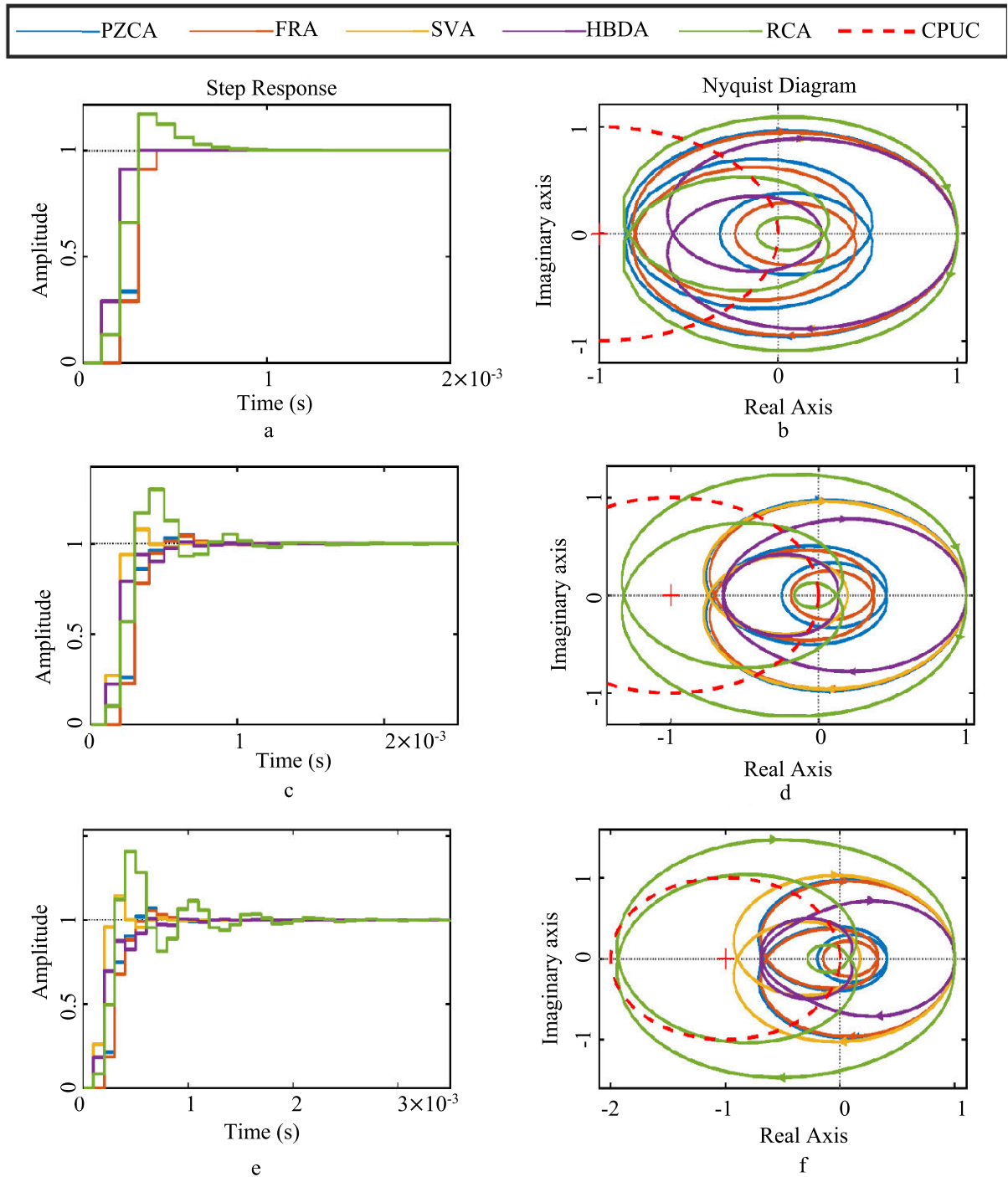
FIGURE 12. Step and Nyquist plots at (a,b) steady state, (c,d) 40% grid-impedance variation and (e,f) 80% grid-impedance variation, respectively.

the poles and zeros into compensable and non-compensable parts to avoid compensating the zeros outside the unit circle. The plant numerator was split to contain B^+ and B^-, which represented compensable and non-compensable zeros, respectively. Using the expression

$$1 - \left(1 - z^{-1}\right) A_{(z)} C_{D(z)} = B^- H_{(z)}$$

polynomials $C_{D(z)}$ and $M_{(z)}$ were chosen arbitrarily to satisfy the control variable constraints. The two polynomials were obtained by comparison as:

$$C_{D(z)} = 1 + 1.21598z^{-1} \quad \text{and}$$

$$H_{(z)} = 1.024z^{-1} - 0.8771z^{-2} + 0.25z^{-3} - 0.060533z^{-4}$$
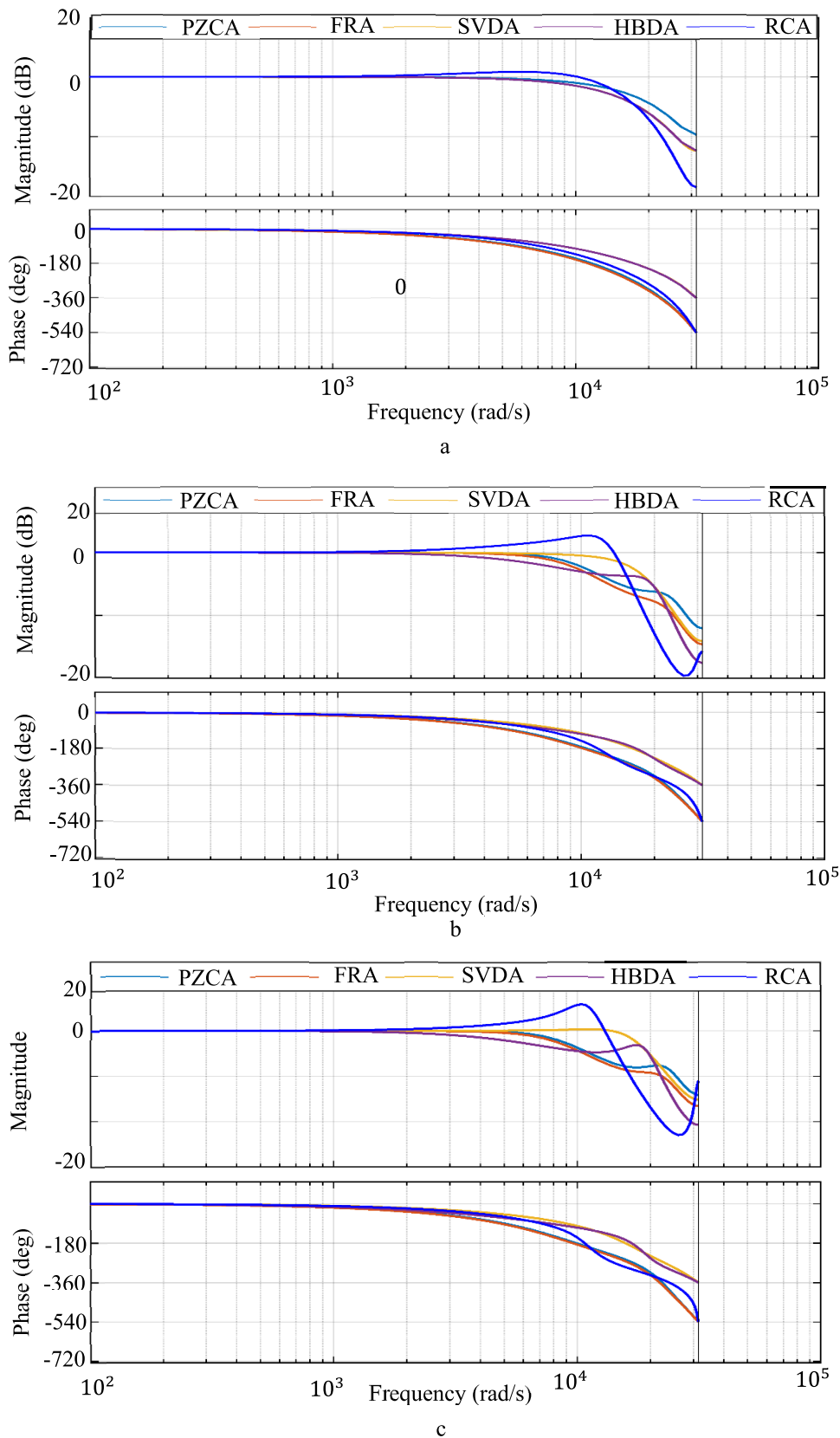
FIGURE 13. Bode plots for PZCA, FRA, SVDA, HBDA, and RCA at (a) steady state, (b) 40% grid-impedance variation and (c) 80% grid-impedance variation. grid impedance variation respecivel.
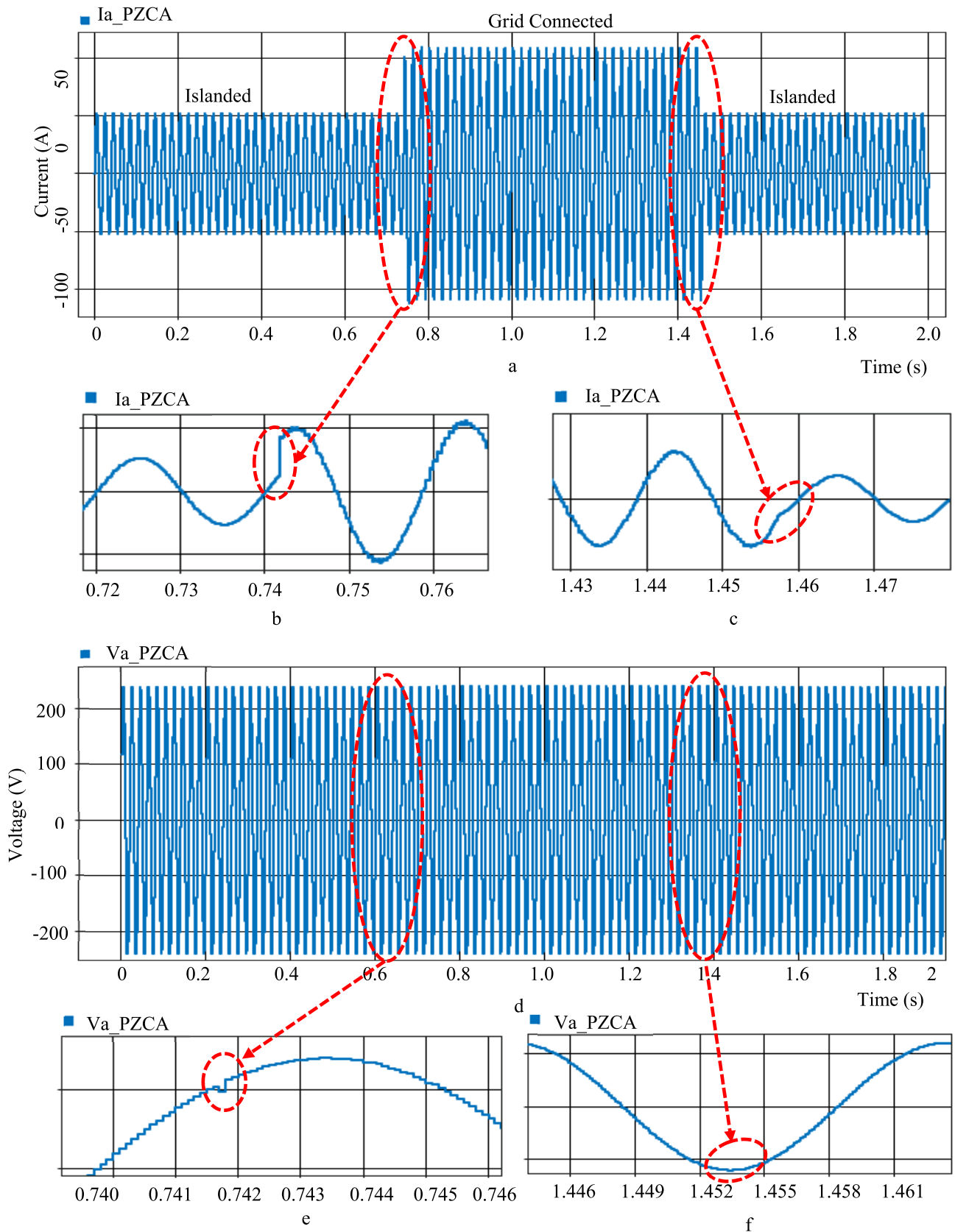
FIGURE 14. Voltage and current of PZCA. (a) Phase A Current at Islanded and Grid mode. (b) Distortion at the transition between Islanded to Grid mode. (c) Distortion at the transition between Grid to Islanded mode. (d) Phase A, Voltage wave form at Islanded and Grid mode. (e) Voltage distortion at the transition from Islanded to Grid. (f) Voltage distortion at the transition from Grid to Islanded.
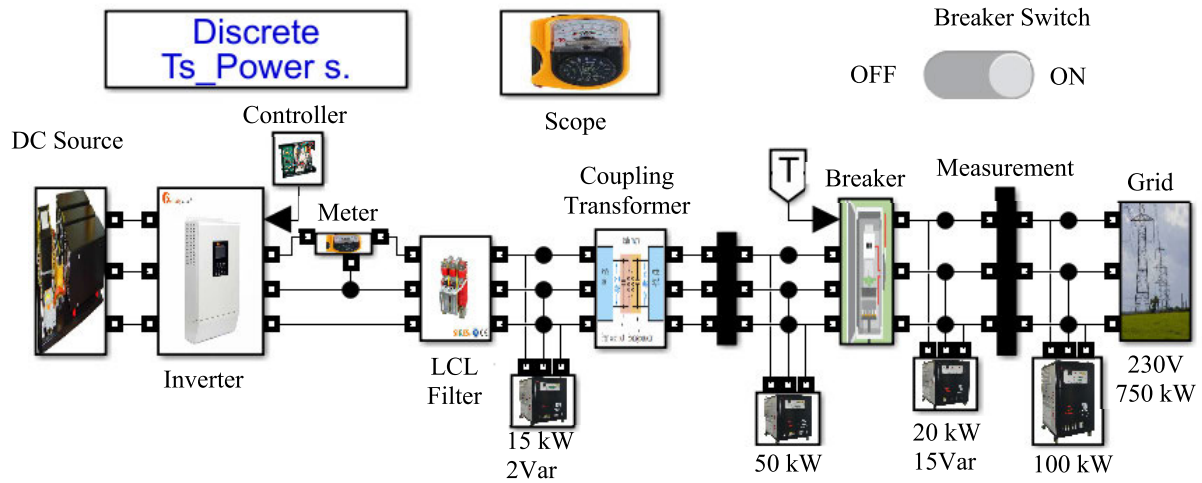
FIGURE 15. Simulation diagram of one of the controllers (PZCA).
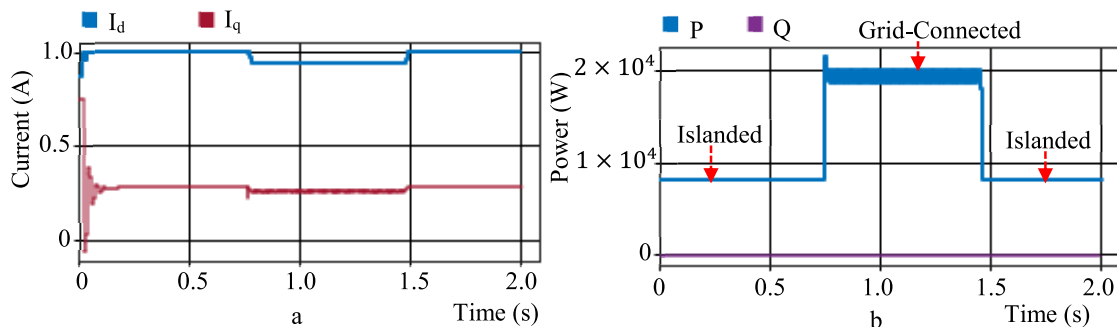
FIGURE 16. (a) I_d and I_q and (b) power output.

The inner-loop deadbeat controller was obtained by substituting the above polynomials into Equation 21, as in Equation 47:

$$DB_{mcn(z)} = \frac{0.66558\,(z - 0.616)\,(z^2 - 0.2405z + 0.09597)}{(z + 1.216)\,(z - 1)\,(z + 0.1526)}$$
(47)

The pre-filter controller was obtained from Equation 22, as in Equation 48:

$$DB_{pf(z)} = \frac{0.13013z\,(z + 1.976)\,(z + 0.1526)}{(z - 0.4882)\,(z^2 - 0.2155z + 0.08774)}$$
(48)

The overall feedback transfer function from the input to the output is given by Equation 49, and the step and Nyquist plots are shown in Subplots (i) and (j), respectively, in Figure 11b. As evident from the plots, the system settled at 12 sampling periods with 17% overshoot, and from the Nyquist plot, there was no encirclement of the critical point, which indicated that the closed-loop system is stable.

$$\frac{Y(z)}{E(z)}$$
$$= \frac{0.13431\,(z + 1.976)^2\,(z - 0.616)\,(z + 0.1526)^2}{z^2\,(z - 0.4882)\,(z + 0.36)\,(z^2 - 0.2155z + 0.08774)}$$
(49)

Table 3 gives a summary of the control laws, and the output difference equation of each of the controllers discussed earlier. Next, we are going to discuss which of the approach is best in terms of stability, especially with regard to grid-impedance variation.

F. RQ3: WHICH APPROACH IS BEST IN TERMS OF STABILITY ESPECIALLY WITH REGARD TO GRID-IMPEDANCE VARIATION?

Figure 12 shows the step and Nyquist plots for the five controllers at steady state, as well as at 40% and 80% grid-impedance fluctuations, to address this question. Despite the variance in impedance, all of the controllers except the RCA displayed moderate or no overshoots, as seen in the step charts. Similarly, none of the Nyquist plots, with the exception of the RCA, showed encirclement of the critical point, indicating that the closed-loop system was stable. The RCA's overshoots and amount of encirclement rose as grid impedance increased, as shown by the Bode plot and the tabulated stability characteristics shown in Figure 13 and Table 4, respectively. According to the Bode plots, all of the controllers' low-frequency asymptotes were at zero decibels (dB) with a flat curve at steady state, as shown in Subplot (a) in Figure 13. This demonstrated the suppression of all resonances. However, there was a

TABLE 4. Stability parameters at different grid-impedance variations.

Controllers	G_m (dB)	P_m (deg)	W_{pc} (rad/s)	W_{gc} (rad/s)	Settling time (s)	Overshoot (%)	Encirclements	Stable or not
At steady state								
PZCA	1.1724	-180	1.1710	0	3	0	None	Stable
FRA	1.2410	-180	1.238	0	4	0	None	Stable
HBDA	1.6940	-180	1.7441	0	3	0	None	Stable
SVDA	1.6940	-180	1.7441	0	3	0	None	Stable
RCA	1.1827	44.0	1.3203	1.0266	12	17	None	Stable
At 40% grid-impedance variation								
PZCA	1.3634	-180	1.0647	0	10	5	None	Stable
FRA	1.4167	-180	1.0262	0	12	4	None	Stable
HBDA	1.5477	-180	1.6918	0	14	1	None	Stable
SVDA	1.3404	-180	1.6384	0	8	8	None	Stable
RCA	0.7576	-45	1.1751	1.3622	-	32	2	Not stable
At 80% grid-impedance variation								
PZCA	1.5123	-180	0.9901	0	15	7	None	Stable
FRA	1.5590	-180	0.9572	0	14	6	None	Stable
HBDA	1.4554	-180	1.6723	0	34	3	None	Stable
SVDA	1.1148	29	1.5738	1.3816	12	15	None	Stable
RCA	0.5160	-70	1.0722	1.2968	-	43	2	Not stable

Note: G_m: gain margin, P_m: phase margin, W_{pc}: phase cross-over frequency, W_{gc}: gain cross-over frequency

peak from the RCA in Subplots (b) and (c), indicating the existence of certain resonance frequencies. Elaborate simulations using the five controllers were carried out, with an example of the simulation diagram illustrated in Figure 15, to test these control techniques further. An identical configuration was created for the five controllers; however, only one of the setups, the PZCA, is shown due to picture quality concerns.

In addition, Figure 14's Subplot (a) depicts the current at the point of common coupling (PCC) before and after the current injection, as shown in Subplots (b) and (c), respectively. The voltage at the PCC in islanded and grid-connected modes is shown in Subplot (d). Subplots (e) and (f) depict the distortions caused by hooking and falling off the grid, respectively. The aberrations for both current and voltage were clearly within permissible limits. Figures 16(a) and (b) illustrate the current controller's direct-quadrature-zero (dq0) currents and the power injected into the grid by the inverter, respectively. The 80kW inverter pushed around 12 kW of electricity into the grid, as seen from the plot. Table 5 shows the THDs of these controllers at the designed sampling and switching frequencies of 10 kHz, whereas Table 6 shows the THDs at alternative frequencies, such as 100 kHz sampling and 10 times the designed sample frequency. This further verified that these controllers can work perfectly with sampling and switching frequencies that were different from the designed one. Figure 17 depicts a visual depiction of the current's total harmonic distortion from the controllers at steady state with the designed sampling and switching frequencies.

The stability parameters from Table 4 and the summary of current and voltage total harmonic distortion from Tables 5 and 6 were examined to answer this research question, and it was discovered that the state-variable derivation approach showed an outstanding response both at steady state and at transient time due to the grid-impedance variation. As a result, it may be argued that it is the most effective strategy.

G. RQ4: WHAT ARE THE BARRIERS THAT MAY PREVENT THE WIDE ADOPTION OF DBCC IN GCIAs?

To address the fourth research question, the practical issues of each of the methods presented are discussed here. DBC has been criticized because of its aggressivity. This aggressivity makes this controller less robust against model error and noise in practical implementation. However, this type of controller has some desirable applications especially when the error or noise is small, for example, as a state observer, model-based feed-forward control and model-based feedback control. Additionally, it could be useful in a simulation environment and of great benefit in the academic teaching environment because DBC accomplishes settling that could not be achieved otherwise. The achievements include complete suppression of asymptotic decay and reaching the finite state in the shortest possible time. Next, we are going to discuss in brief the issues with each of the methods.

1) ISSUES WITH POLE-ZERO CANCELLATION APPROACH

For the case of all-discrete components (controller and plant), this method produced a minimum-order and minimum-time DBC. Still, for the case of sampled data (digital controller and continuous plant), DBC based on pole and zero cancellations lead to undesirable inter-sampling ripples at the system's output. This is because when plant zeros are canceled, the dynamics of the continuous system are highly excited by the

TABLE 5. Summary of I_THD and V_THD at different grid-impedance variations with f_s and f_{sw} at 10 kHz.

At steady state with f_s and f_{sw} at $10\ kHz$				
Approaches	I_THD (%)	Current (A)	V_THD	Voltage (V)
PZCA	2.35	106.4	0.28	240.5
FRA	2.35	106.4	0.27	240.5
SVDA	2.44	109.2	0.26	240.5
HBDA	3.41	96.14	0.26	240.5
RCA	22.18	76.71	0.23	240.2
At 40% grid-impedance variation with f_s and f_{sw} at $10kHz$				
PZCA	2.44	106.7	0.18	240.4
FRA	2.44	106.7	0.18	240.4
SVDA	2.46	109.6	0.17	240.4
HBDA	3.52	94.23	0.15	240.3
RCA	23.80	77.1	0.15	240.2
At 80% grid-impedance variation with f_s and f_{sw} at $10kHz$				
PZCA	2.49	107	0.06	240.2
FRA	2.49	107	0.06	240.2
SVDA	2.28	109.1	0.06	240.3
HBDA	3.52	94.21	0.05	240.2
RCA	28.82	93.25	0.05	240.2
Note:f_s : sampling frequency, f_{sw}: switching frequency, THD: total harmonic distortion				

TABLE 6. Summary of I_THD and V_THD at different grid-impedance variations with $f_s = 100$ kHz and $f_{sw} = 10* f_s$.

At steady state with f_s =100 kHz and $f_{sw} = 10 * f_s$				
Approach	I_THD (%)	Current (A)	V_THD	Voltage (V)
PZCA	1.00	107.7	0.13	240.5
FRA	1.00	107.7	0.13	240.5
SVDA	1.04	108.7	0.13	240.5
HBDA	4.67	42.53	0.23	240.4
RCA	17.52	82.61	0.17	240.2
At 40% grid-impedance variation with $f_s = 100$ kHz and $f_{sw} = 10 * f_s$				
PZCA	1.00	107.9	0.08	240.4
FRA	1.03	108	0.08	240.4
SVDA	1.07	108.8	0.09	240.4
HBDA	4.73	42.73	0.14	240.3
RCA	21.72	78.03	0.11	240.2
At 80% grid-impedance variation with $f_s = 100$ kHz and $f_{sw} = 10 * f_s$				
PZCA	1.05	107.6	0.03	240.2
FRA	1.04	108	0.03	240.2
SVDA	1.08	108.7	0.03	240.2
HBDA	4.89	42.95	0.05	240.3
RCA	21.45	78.54	0.04	240.2
Note:f_s: sampling frequency, f_{sw}: switching frequency, THD: total harmonic distortion				

input and, at the same time, are not affected by the available feedback [17].

2) ISSUES WITH FACTORIZATION APPROACH

This approach's control signal is always high, which means much energy is needed to drive the system to the steady state within the shortest possible time. However, when the control signal is constrained to some lower values, the controller's speed is compromised. Therefore, there is always a tradeoff between speed and the energy needed by the control signal.

3) ISSUES WITH STATE-VARIABLE DERIVATION APPROACH

The fast convergence in this method is achieved at the expense of an aggressive input. Additionally, this method requires more systematic design procedures than just placing the poles.
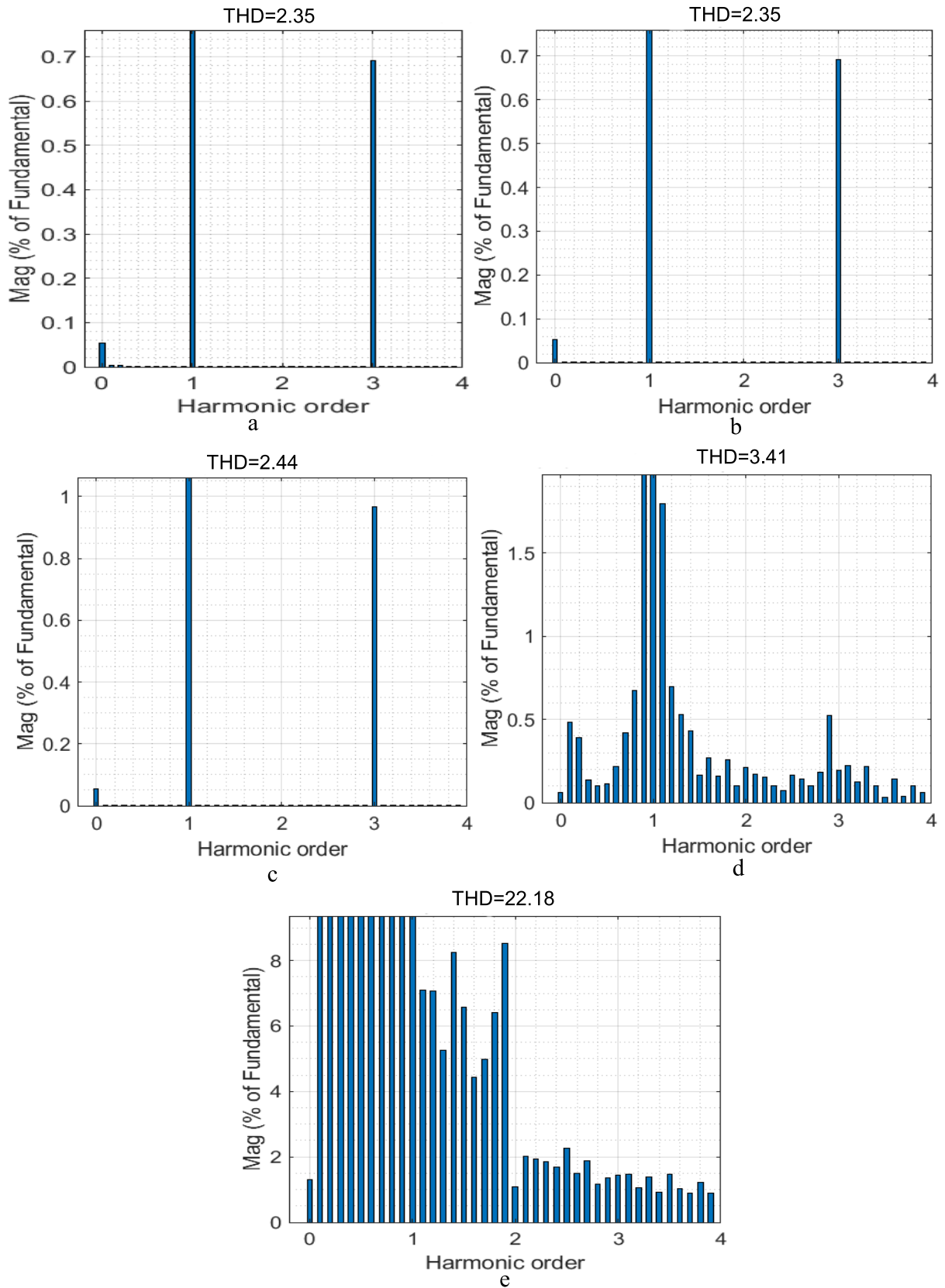
FIGURE 17. CTHD of (a) PZCA, (b) FRA, (c) SVDA, (d) HBDA and (e) RCA.

4) ISSUES WITH HYBRID DBC USING STATE-SPACE DESIGN APPROACH

The fast convergence in this method is achieved at the expense of an aggressive input, as in the previous case. Additionally, this method requires more systematic design procedures than just placing the poles with the control error's integration.

5) ISSUES WITH ROBUST DESIGN APPROACH

In the case of a controller with a pre-filter, the design is simple and straightforward, but there is an increase in the order of the controller, in addition to the increase in the cost of the sensors required. Therefore, the reliability of this control approach is less compared with the other types.

IV. CONCLUSION

In this paper, the analytical contribution from previous research on DBCC used in grid-connected inverters has been systematically summarized. This review paper has answered four critical research questions. The first was the evidence that indicated the adoption of DBC in GCIAs, wherein a literature classification was systematically created, which confirmed a final sample of 54 papers. One can conclude that there is an increase in the adoption of these controllers. The second question addressed the types of DBC approaches adopted in GCIAs, and theories and illustrative examples of different classes of DBC were presented to give the readers a summary of prominent approaches in this area of research. The third question addressed which approach is the best in terms of stability, especially regarding the grid-impedance variation. Theoretical analysis of the controller, as well as intensive simulations, has been conducted as presented in the previous sections. It was established that the SVDA approach shows outstanding fast step response and better stability gain and phase margin as well as a lower THD despite the variation in the grid impedance. The final question addressed the barriers that might prevent the wide adoption of DBCC in GCIAs. It was established that this type of controller has been criticized because of its aggressivity and lack of robustness to parameter variation and noise. However, it was presented earlier that the aggressivity can be lessened by using the turning polynomial at the expense of increasing the time for the system to settle. Careful design of the controller with the correct tuning polynomials can improve its robustness against parameter variation. In summary, the main contribution of this research work was to summarize and evaluate the existing literature on deadbeat control techniques in grid-connected inverter applications. In conclusion, the deadbeat current control is a promising control method when the right tunning polynomials are used. Conducting experimental tests to validate further the intensive simulation conducted here could be a direction for further research.

ACKNOWLEDGMENT

REFERENCES

[1] M. A. R. Haider, S. A. Saleh, R. Shao, and L. Chang, "Robust current controller for grid-connected voltage source inverter," in *Proc. IEEE 8th Int. Symp. Power Electron. Distrib. Gener. Syst. (PEDG)*, Apr. 2017, pp. 1–7, doi: 10.1109/PEDG.2017.7972500.

[2] G. Elhassan, S. A. Zulkifli, E. Pathan, M. H. Khan, and R. Jackson, "A comprehensive review on time-delay compensation techniques for grid-connected inverters," *IET Renew. Power Gener.*, vol. 15, no. 2, pp. 251–256, Nov. 2021, doi: 10.1049/rpg2.12033.

[3] Y. A.-R. I. Mohamed and E. F. El-Saadany, "An improved deadbeat current control scheme with a novel adaptive self-tuning load model for a three-phase PWM voltage-source inverter," *IEEE Trans. Ind. Electron.*, vol. 54, no. 2, pp. 747–759, Apr. 2007, doi: 10.1109/TIE.2007.891767.

[4] M. G. Judewicz, S. A. González, J. R. Fischer, J. F. Martínez, and D. O. Carrica, "Inverter-side current control of grid-connected voltage source inverters with LCL filter based on generalized predictive control," *IEEE J. Emerg. Sel. Topics Power Electron.*, vol. 6, no. 4, pp. 1732–1743, Dec. 2018, doi: 10.1109/JESTPE.2018.2826365.

[5] M. Pichan, H. Rastegar, and M. Monfared, "A new digital control of four-leg inverters in the natural reference frame for renewable energy-based distributed generation," *Int. Trans. Electr. Energy Syst.*, vol. 29, no. 5, 2019, Art. no. e2836, doi: 10.1002/2050-7038.2836.

[6] T. T. Hartley, R. J. Veillette, and G. Cook, "Techniques in deadbeat and one-step-ahead control," *Control Dyn. Syst.*, vol. 79, no. C, pp. 117–157, 1996, doi: 10.1016/S0090-5267(96)80006-5.

[7] R. W. Longman and M. Q. Phan, "Iterative learning control as a method of experiment design for improved system identification," *Optim. Methods Softw.*, vol. 21, no. 6, pp. 919–941, Dec. 2006, doi: 10.1080/10556780600881431.

[8] R. A. Bergen and R. J. Ragazzini, "Sampled-data processing techniques for feedback control systems," *Trans. Amer. Inst. Electr. Eng., Appl. Ind.*, vol. 73, no. 5, pp. 236–247, Nov. 1954, doi: 10.1109/tai.1954.6371426.

[9] C. A. Busada, S. G. Jorge, and J. A. Solsona, "A synchronous reference frame PI current controller with dead beat response," *IEEE Trans. Power Electron.*, vol. 35, no. 3, pp. 3097–3105, Mar. 2020, doi: 10.1109/TPEL.2019.2925705.

[10] J. Kim, J. Hong, and H. Kim, "Improved direct deadbeat voltage control with an actively damped inductor-capacitor plant model in an islanded AC microgrid," *Energies*, vol. 9, no. 11, p. 978, Nov. 2016, doi: 10.3390/en9110978.

[11] J. Wang, Y. Tang, Y. Qi, P. Lin, and Z. Zhang, "A unified startup strategy for modular multilevel converters with deadbeat predictive current control," *IEEE Trans. Ind. Electron.*, vol. 68, no. 8, pp. 6401–6411, Aug. 2021, doi: 10.1109/TIE.2020.3007080.

[12] J. C. Moreno, J. M. E. Huerta, R. G. Gil, and S. A. González, "A robust predictive current control for three-phase grid-connected inverters," *IEEE Trans. Ind. Electron.*, vol. 56, no. 6, pp. 1993–2004, Jun. 2009, doi: 10.1109/TIE.2009.2016513.

[13] Y. A. M. Qasem, R. Abdullah, Y. Y. Jusoh, R. Atan, and S. Asadi, "Cloud computing adoption in higher education institutions: A systematic review," *IEEE Access*, vol. 7, pp. 63722–63744, 2019, doi: 10.1109/ACCESS.2019.2916234.

[14] A. F. Alshalif, J. M. Irwan, N. Othman, A. A. Al-Gheethi, and S. Shamsudin, "A systematic review on bio-sequestration of carbon dioxide in bio-concrete systems: A future direction," *Eur. J. Environ. Civil Eng.*, vol. 4, pp. 1–20, Feb. 2020, doi: 10.1080/19648189.2020.1713899.

[15] V. Kuera, "A dead-beat servo problem," *Int. J. Control*, vol. 32, no. 1, pp. 107–113, Jul. 1980, doi: 10.1080/00207178008922847.

[16] W. Yao, J. Cui, and W. Yao, "Single-phase inverter deadbeat control with one-carrier-period lag," *Electronics*, vol. 9, no. 1, pp. 1–11, 2020, doi: 10.3390/electronics9010154.

[17] H. Sirisena, "Ripple-free deadbeat control of SISO discrete systems," *IEEE Trans. Autom. Control*, vol. AC-30, no. 2, pp. 168–170, Feb. 1985, doi: 10.1109/tac.1985.1103912.

[18] P. Pariz and M. Monfared, "A deadbeat controller design for single-phase active power filters based on forward-backward discretization," in *Proc. 12th Power Electron. Drive Syst. Technol. Conf. (PEDSTC)*, Feb. 2021, pp. 1–5, doi: 10.1109/PEDSTC52094.2021.9405889.

[19] M. L. Andreu, J. Rohten, and J. Espinoza, "Soft-deadbeat control for multivariable three phase VSC under variable grid voltage," in *Proc. 47th Annu. Conf. Ind. Electron. Soc.*, May 2021, pp. 1–978-6654, doi: 10.1109IECON48115.2021.9589668.

[20] K. Nishida, T. Ahmed, and M. Nakaoka, "Cost-effective deadbeat current control for wind-energy inverter application with LCL filter," *IEEE Trans. Ind. Appl.*, vol. 50, no. 2, pp. 1185–1197, Mar. 2014, doi: 10.1109/TIA.2013.2279900.

[21] T. Ahmed, K. Nishida, and I. Nanno, "State-vector feedback gain analysis for deadbeat control of grid-integrated inverter with LCL filter," in *Proc. 18th Eur. Conf. Power Electron. Appl. (EPE ECCE Europe)*, Sep. 2016, pp. 1–9, doi: 10.1109/EPE.2016.7695651.

[22] Y. A. R. I. Mohamed and E. F. El-Saadany, "A control scheme for PWM voltage-source distributed-generation inverters for fast load-voltage regulation and effective mitigation of unbalanced voltage disturbances," *IEEE Trans. Ind. Electron.*, vol. 55, no. 5, pp. 2453–2459, 2008, doi: 10.1109/PESC.2008.4592309.

[23] G. Zhao, J. Ma, L. Huang, and Y. Tang, "Investigation of reducing the influence of digital control delay to LCL-type grid-connected inverter," in *Proc. IEEE Energy Convers. Congr. Expo.*, Apr. 2016, pp. 1–6, doi: 10.1109/ECCE.2016.7855219.

[24] Y. A. R. I. Mohamed and E. F. El-Saadany, "A control method of grid-connected PWM voltage source inverters to mitigate fast voltage disturbances," *IEEE Trans. Power Syst.*, vol. 24, no. 1, pp. 489–491, Feb. 2009, doi: 10.1109/TPWRS.2008.2006996.

[25] Y. A.-R.-I. Mohamed and E. F. El-Saadany, "Robust high bandwidth discrete-time predictive current control with predictive internal model—A unified approach for voltage-source PWM converters," *IEEE Trans. Power Electron.*, vol. 23, no. 1, pp. 126–136, Jan. 2008, doi: 10.1109/TPEL.2007.911797.

[26] Q. Zeng and L. Chang, "An advanced SVPWM-based predictive current controller for three-phase inverters in distributed generation systems," *IEEE Trans. Ind. Electron.*, vol. 55, no. 3, pp. 1235–1246, Mar. 2008, doi: 10.1109/TIE.2007.907674.

[27] J. R. Fischer, S. A. Gonzalez, M. A. Herran, M. G. Judewicz, and D. O. Carrica, "Calculation-delay tolerant predictive current controller for three-phase inverters," *IEEE Trans. Ind. Informat.*, vol. 10, no. 1, pp. 233–242, Feb. 2014, doi: 10.1109/TII.2013.2276104.

[28] X. Li, J. Chen, and J. Zhang, "Three-phase Z-source grid-connected wind power generation system based on novel deadbeat control," in *Proc. 2nd Int. Conf. Digit. Manuf. Autom. (ICDMA)*, 2011, pp. 1355–1359, 2011, doi: 10.1109/ICDMA.2011.333.

[29] V. R. Chowdhury and J. W. Kimball, "Adaptive control of a three-phase grid-connected inverter with near deadbeat response," in *Proc. Appl. Power Electron. Conf. Expo.*, 2021, pp. 2698–2701, doi: 10.1109/APEC42165.2021.9486983.

[30] M. H. Durgante and M. Stefanello, "Multi loop deadbeat+repetitive and adaptive control for power converters with LCL filters," in *Proc. 38th Annu. Conf. Ind. Electron. Soc.*, Oct. 2012, pp. 5955–5960, doi: 10.1109/IECON.2012.6389108.

[31] Y. Tao, C. Tan, Q. Chen, L. Zhang, K. Zhou, and L. Liu, "Deadbeat repetitive control for a grid-connected inverter with LCL filter," in *Proc. IEEE 15th Int. Conf. Control Autom. (ICCA)*, Jul. 2019, pp. 573–577, doi: 10.1109/ICCA.2019.8899637.

[32] K. Fouad, H. M. Boulouiha, A. Allali, A. Taibi, and M. Denai, "Multivariable control of a grid-connected wind energy conversion system with power quality enhancement," *Energy Syst.*, vol. 9, no. 1, pp. 25–57, Feb. 2018, doi: 10.1007/s12667-016-0223-7.

[33] H. Bevrani, B. Franáois, and T. Ise, *Microgrid Dynamics and Control*. Hoboken, NJ, USA: Wiley, 2017.

[34] Y. Chen, A. Luo, Z. Shuai, and S. Xie, "Robust predictive dual-loop control strategy with reactive power compensation for single-phase grid-connected distributed generation system," *IET Power Electron.*, vol. 6, no. 7, pp. 1320–1328, Aug. 2013, doi: 10.1049/iet-pel.2013.0011.

[35] Y. Zhao and H. Kimura, "Dead-beat control with robustness," *Int. J. Control*, vol. 43, no. 5, pp. 1427–1440, May 1986, doi: 10.1080/00207178608933549.

[36] E. Zafiriou and M. Morari, "Digital controllers for SISO systems: A review and a new algorithm," *Int. J. Control*, vol. 42, no. 4, pp. 855–876, 1985, doi: 10.1080/00207178508933400.

[37] Y. Xing, C. Tan, Q. Chen, L. Zhang, and K. Zhou, "An improved deadbeat plus plug-in repetitive controller for three-phase four-leg inverters," in *Proc. 43rd Annu. Conf. Ind. Electron. Soc.*, Oct. 2017, pp. 6325–6329, doi: 10.1109/IECON.2017.8217101.

[38] J. M. E. Huerta, J. Castello, J. R. Fischer, and R. Garcia-Gil, "A synchronous reference frame robust predictive current control for three-phase grid-connected inverters," *IEEE Trans. Ind. Electron.*, vol. 57, no. 3, pp. 954–962, Mar. 2010, doi: 10.1109/TIE.2009.2028815.

[39] J. M. Espi, J. Castello, R. García-Gil, G. Garcera, and E. Figueres, "An adaptive robust predictive current control for three-phase grid-connected inverters," *IEEE Trans. Ind. Electron.*, vol. 58, no. 8, pp. 3537–3546, Aug. 2011, doi: 10.1109/TIE.2010.2089945.

[40] Y. Chen and A. Luo, "A robust predictive dual-loop control strategy for grid-connected photovoltaic generation system," in *Proc. 7th Int. Power Electron. Motion Control Conf.*, Jun. 2012, pp. 2007–2011, doi: 10.1109/IPEMC.2012.6259149.

[41] H.-S. Heo, G.-H. Choe, and H.-S. Mok, "Robust predictive current control of a grid-connected inverter with harmonics compensation," in *Proc. 28th Annu. Appl. Power Electron. Conf. Expo.*, Oct. 2013, pp. 2212–2217, doi: 10.1109/APEC.2013.6520602.

[42] L. Yang, A. Luo, Y. Chen, K. Huai, and L. Zhou, "A fast robust PWM method for photovoltaic grid-connected inverter," in *Proc. 43rd Annu. Conf. Ind. Electron. Soc.*, Jan. 2017, pp. 4811–4816, doi: 10.1109/IECON.2017.8216830.

[43] T. T. Hartley and A. D. Sarantopoulos, "Using feedthrough for near one-step-ahead control of inversely unstable plants," *IEEE Trans. Autom. Control*, vol. 36, no. 5, pp. 625–627, May 1991, doi: 10.1109/9.76369.

[44] R. Ottersten and J. Svensson, "Vector current controlled voltage source converter-deadbeat control and saturation strategies," *IEEE Trans. Power Electron.*, vol. 17, no. 2, pp. 279–285, Mar. 2002, doi: 10.1109/63.988947.

[45] A. Timbus, M. Liserre, R. Teodorescu, P. Rodriguez, and F. Blaabjerg, "Evaluation of current controllers for distributed power generation systems," *IEEE Trans. Power Electron.*, vol. 24, no. 3, pp. 654–664, Mar. 2009, doi: 10.1109/TPEL.2009.2012527.

[46] W. Jiang, W. Ma, J. Wang, L. Wang, and Y. Gao, "Deadbeat control based on current predictive calibration for grid-connected converter under unbalanced grid voltage," *IEEE Trans. Ind. Electron.*, vol. 64, no. 7, pp. 5479–5491, Jul. 2017, doi: 10.1109/TIE.2017.2674620.

[47] Y. A.-R.-I. Mohamed, "Suppression of low and high-frequency instabilities and grid-induced disturbances in distributed generation inverters," *IEEE Trans. Power Electron.*, vol. 26, no. 12, pp. 3790–3803, Dec. 2011, doi: 10.1109/TPEL.2011.2161489.

[48] Y. A.-R. I. Mohamed, M. A. Rahman, and R. Seethapathy, "Robust line-voltage sensorless control and synchronization of LCL-filtered distributed generation inverters for high power quality grid connection," *IEEE Trans. Power Electron.*, vol. 27, no. 1, pp. 87–98, Jan. 2012, doi: 10.1109/TPEL.2011.2159866.

[49] J. S. Lim, C. Park, J. Han, and Y. I. Lee, "Robust tracking control of a three-phase DC-AC inverter for UPS applications," *IEEE Trans. Ind. Electron.*, vol. 61, no. 8, pp. 4142–4151, Aug. 2014, doi: 10.1109/TIE.2013.2284155.

[50] S. Buso, T. Caldognetto, and Q. Liu, "Analysis and experimental characterization of a large-bandwidth triple-loop controller for grid-tied inverters," *IEEE Trans. Power Electron.*, vol. 34, no. 2, pp. 1936–1949, Feb. 2019, doi: 10.1109/TPEL.2018.2835158.

[51] Z. Zeng, H. Yang, R. Zhao, and C. Cheng, "Topologies and control strategies of multi-functional grid-connected inverters for power quality enhancement: A comprehensive review," *Renew. Sustain. Energy Rev.*, vol. 24, pp. 223–270, Aug. 2013, doi: 10.1016/j.rser.2013.03.033.

[52] Z. Fu, H. Xie, J. Xue, H. Luo, and Z. Lin, "Research on improved deadbeat control strategy based on interpolation prediction and online inductance identification," *J. Electr. Comput. Eng.*, vol. 2020, pp. 1–13, Jan. 2020, doi: 10.1155/2020/3164034.

[53] P. Yang, N. Chen, and S. Liu, "Research on the improved current deadbeat control algorithm of photovoltaic grid-connected inverter," in *Proc. 4th Int. Conf. Power Electron. Syst. Appl.*, vol. 3, 2011, pp. 1–5, doi: 10.1109/PESA.2011.5982948.

[54] L. Wang, N. Ertugrul, and M. Kolhe, "Evaluation of dead beat current controllers for grid-connected converters," in *Proc. IEEE Innov. Smart Grid Technol.*, May 2012, pp. 1–7, doi: 10.1109/ISGT-Asia.2012.6303109.

[55] C. R. D. Osorio, G. S. Da Silva, J. C. Giacomini, and C. Rech, "Comparative analysis of predictive current control techniques applied to single-phase grid-connected inverters," in *Proc. 14th Brazilian Power Electron. Conf.*, Jun. 2017, pp. 1–6, doi: 10.1109/COBEP.2017.8257329.

[56] J. A. Rohten, D. N. Dewar, P. Zanchetta, A. Formentini, J. A. Muñoz, C. R. Baier, and J. J. Silva, "Multivariable deadbeat control of power electronics converters with fast dynamic response and fixed switching frequency," *Energies*, vol. 14, no. 2, p. 313, Jan. 2021, doi: 10.3390/en14020313.

[57] A. Zama, A. Benchaib, S. Bacha, D. Frey, S. Silvant, and D. Georges, "Linear feedback dead-beat control for modular multilevel converters: Validation under faults grid operation mode," *IEEE Trans. Ind. Electron.*, vol. 68, no. 4, pp. 3181–3191, Apr. 2021, doi: 10.1109/TIE.2020.2978708.

[58] Z. Wang and L. Chang, "A hybrid control method for three-phase grid-connected inverters with high quality power," in *Proc. IEEE Energy Convers. Congr. Expo. ECCE*, Apr. 2009, pp. 17–24, doi: 10.1109/ECCE.2009.5316309.

[59] H. Zhang, H. Zhou, J. Ren, W. Liu, S. Ruan, and Y. Gao, "Three-phase grid-connected photovoltaic system with SVPWM current controller," in *Proc. IEEE 6th Int. Power Electron. Motion Control Conf. (IPEMC)*, Dec. 2009, vol. 9, vol. 3, pp. 2161–2164, doi: 10.1109/IPEMC.2009.5157759.

[60] S. Wei, Z. Zhao, K. Li, L. Yuan, and W. Wen, "Deadbeat current controller for bidirectional dual-active-bridge converter using an enhanced SPS modulation method," *IEEE Trans. Power Electron.*, vol. 36, no. 2, pp. 1274–1279, Feb. 2021, doi: 10.1109/TPEL.2020.3007706.

[61] N. Bekhoucha, M. Kermadi, N. Mesbahi, and S. Mekhilef, "Performance investigation of deadbeat predictive controllers for three-level neutral point clamped inverter," *IEEE J. Emerg. Sel. Top. Power Electron.*, early access, Jun. 24, 2021, doi: 10.1109/JESTPE.2021.3092057.

[62] J. Chen, H. Shao, and C. Liu, "An improved deadbeat control strategy based on repetitive prediction against grid frequency fluctuation for active power filter," *IEEE Access*, vol. 9, pp. 24646–24657, 2021, doi: 10.1109/ACCESS.2021.3057386.

[63] L. Zhou, M. Yang, Q. Liu, and K. Guo, "New control strategy for three-phase grid-connected LCL inverters without a phase-locked loop," *J. Power Electron.*, vol. 13, no. 3, pp. 487–496, May 2013, doi: 10.6113/JPE.2013.13.3.487.

[64] Y. Tang, P. C. Loh, P. Wang, F. H. Choo, F. Gao, and F. Blaabjerg, "Generalized design of high performance shunt active power filter with output LCL filter," *IEEE Trans. Ind. Electron.*, vol. 59, no. 3, pp. 1443–1452, Mar. 2012, doi: 10.1109/TIE.2011.2167117.

[65] A. Reznik, M. G. Simões, A. Al-Durra, and S. M. Muyeen, "LCL filter design and performance analysis for grid-interconnected systems," *IEEE Trans. Ind. Appl.*, vol. 50, no. 2, pp. 1225–1232, Mar. 2014, doi: 10.1109/TIA.2013.2274612.

SHAMSUL AIZAM ZULKIFLI was born in Kajang, Selangor, Malaysia. He received the B.S. and M.Sc. degrees from the Universiti Putra Malaysia (UPM), in 2003 and 2006, respectively, and the Ph.D. degree in control system engineering from Loughborough University, U.K., in 2012. He is currently an Associate Professor with the Department of Electrical Power Engineering, Faculty of Electrical and Electronic Engineering, Universiti Tun Hussein Onn Malaysia (UTHM). His research interests include robust control system on power electronics application, and parallel inverter application and smart grid topology for inverter-grid connection. More information can be found at: https://sites.google.com/site/acul1508/.

SOLOMON ZAKWOI ILIYA (Member, IEEE) received the Ph.D. degree from the Wireless Communication Center (WCC), Universiti Teknologi Malaysia (UTM), Johor Bahru, Johor, Malaysia. He attended the Beijing Institute of Tracking and Telecommunications Technology (BITTT), Beijing, China, and the Federal University of Technology Minna, Minna, Nigeria, for his postgraduate and undergraduate studies, respectively. He has over 12 years of experience in his field of study. He is currently the Deputy Director Engineer at the Center for Satellite Technology Development (CSTD), an Activity Arm of the National Space Research and Development Agency (NASRDA). His research interests include microwave, antenna and satellite subsystems designs, and among others. He is a Registered and an Active Member of the Nigerian Society of Engineers (NSE) as well as the Council for the Regulation of Engineering in Nigeria (COREN).

GARBA ELHASSAN was born in Gombe, Nigeria, in 1985. He received the B.Eng. degree (Hons.) in electrical and electronics engineering from the Federal University of Technology, Yola, in 2011, and the Master of Engineering degree from Bayero University, Kano, Nigeria, in 2017. He is currently pursuing the Ph.D. degree with the Universiti Tun Hussein Onn Malaysia. Since 2013, he has been a Staff of the National Space Research and Development Agency, Nigeria. His current research interests include robust deadbeat control system on power electronics applications and dc–dc converter topologies for grid-connected applications.

HASSAN BEVRANI (Senior Member, IEEE) received the Ph.D. degree in electrical engineering from Osaka University, Osaka, Japan, in 2004. He is currently a Full Professor and a Program Leader of the Smart/Micro Grids Research Center (SMGRC), University of Kurdistan (UOK), Sanandaj, Iran. Over the years, he worked as a Senior Research Fellow and a Visiting Professor with Osaka University, Kumamoto University, Japan; the Queensland University of Technology, Australia; the Kyushu Institute of Technology, Japan; Centrale Lille, France; and the Technical University of Berlin, Germany. He is the author of six international books, 15 book chapters, and more than 300 journal articles/conference papers. His current research interests include smart grid operation and control, power systems stability and optimization, microgrid dynamics and control, and intelligent/robust control applications in the power electric industry.

MOMOH KABIR was born in Lagos, Nigeria, in 1982. He received the B.Eng. degree (Hons.) in electrical and electronic engineering from Ambrose Alli University, Ekpoma, Nigeria, in 2008, and the master's degree in electronic and computer engineering from Lagos State University, Lagos, in 2019. He is currently pursuing the Ph.D. degree with the Universiti Tun Hussein Onn Malaysia. His current research interests include power electronics converters, robust control systems, grid stability improvement, and fast electric charging station.

MUBASHIR HAYAT KHAN was born in Bagh, Azad Jammu and Kashmir (AJ&K), Pakistan. He received the B.Sc. (Hons.) and M.S. degrees from the Mirpur University of Science and Technology, AJ&K, in 2008 and 2012, respectively. From 2008 to 2014, he had been associated with Huawei Technologies (Pvt.) Ltd., Hydro-Electric Board of AJ&K, NESPAK (Pvt.) Ltd., and PEL (Pvt.) Ltd. In 2014, he joined the Department of Electrical Engineering, Faculty of Engineering and Technology, University of Poonch Rawalakot (UPR), as a Lecturer. Since 2019, he has been working as a Ph.D. Research Scholar at the Faculty of Electrical Engineering, University Tun Hussein Onn Malaysia. His research interest includes inverter-based smart grid control.

RONALD JACKSON was born in Sarawak, Malaysia, in 1991. He received the B.Eng. (Hons.) and M.Sc. degrees in electrical engineering from the Universiti Tun Hussein Onn Malaysia, Johor, Malaysia, in 2017 and 2019, respectively, where he is currently pursuing the Ph.D. degree. His current research interests include microgrid control, power flow control, self-synchronization, and smart grid applications.

MOHAMMED AHMED was born in Misau. He attended the Federal Polytechnic Staff School Bauchi, Government Science Secondary School Toro in Bauchi State, Abubakar Tafawa Balewa University (ATBU), Bauchi, Nigeria, and Universiti Tun Hussein Onn Malaysia (UTHM). He currently works as the Academic Staff with the Department of Electrical and Electronics Engineering, Abubakar Tafawa Balewa University, Bauchi.

● ● ●